ZSoil

for geotechnics & structures

LARGE DEFORMATIONS

Report 070303

(revised 03.03.2007)

A. Truty
Th. Zimmermann
A. Urbański

GeoDev.

PO Box CH-1001 Lausanne
Switzerland
https://zsoil.com

Contents

Chapter 1

Introduction

ZSoil®2023code is designed to handle large rotations and displacements for all structural elements like shells, beams, membranes, anchors and continuum and large deformations as far as contact interface is concerned. The corotational approach is exploited to manage large rotations and its main benefit is that all the stresses and strains at the integrations points remain the engineering ones although are given in the rotated local frame. The new contact formulation, developed to manage really large relative motions of bodies, makes use of so-called slave-master approach in which contacting node (slave) cannot penetrate the corresponding master element face (master) by means of penalty formulation enhanced by Augmented Lagrangian approach (if needed).

Chapter 2

Co-rotational approach

2.1 Co-rotational approach outline

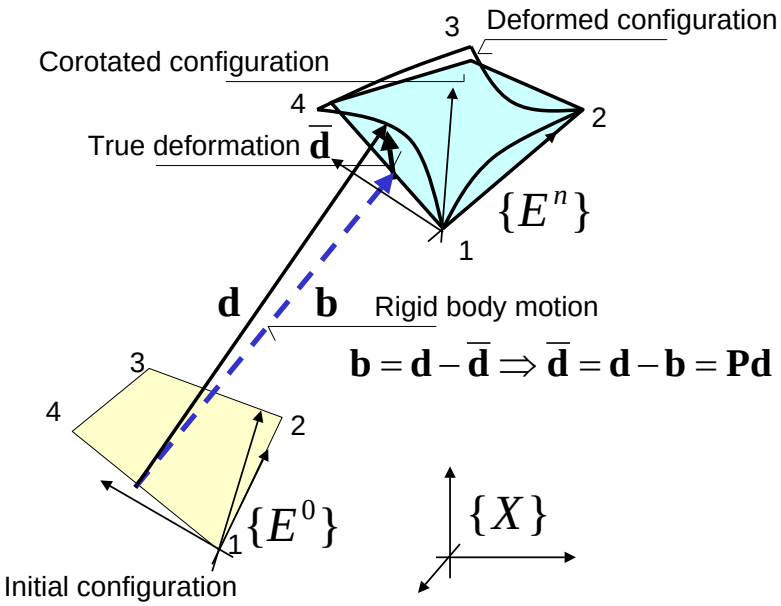

Figure 2.1: Setting element frames

Goal:

to perform **large displacement/rotation** analysis re-utilizing standard geometrically linear element for:

- beams in 2D and 3D
- shells
- membranes
- truss/anchors

Assumption:

Displacements and rotations attributed to rigid body motion could be arbitrarily large, but **"true deformation" remains within small strain limit**

Performance:

- **deduct rigid body motion** from total deformation of an element, then evaluate element forces and stiffness emerging from -"true" -deformation
- introduce of **element frame E** rigidly attached to the element. Element processing is performed with respect to these frame
- deduction of rigid body motion is equivalent to a projection:

$$\begin{aligned}\delta\bar{\mathbf{d}} &= \mathbf{P}\delta\mathbf{d}\\ \mathbf{f} &= \mathbf{P}^{\mathrm{T}}\bar{\mathbf{f}}\\ \mathbf{P} &= \frac{\partial\bar{\mathbf{d}}}{\partial\mathbf{d}}\\ \mathbf{K} &= \mathbf{P}^{\mathrm{T}}\,\bar{\mathbf{K}}\mathbf{P} + \frac{\partial\mathbf{P}^{\mathrm{T}}}{\partial\mathbf{d}}\bar{\mathbf{f}}\end{aligned}$$

- consistent treatment of arbitrarily large rotation:
  - ⋆ representation of a rotation by the tensor, use exponential mapping (Rodriguez formula):

$$\text{orthogonal tensor } \mathbf{Q} \;\underset{\boldsymbol{\Omega}=\log\mathbf{Q}}{\overset{\mathbf{Q}=e^{\boldsymbol{\Omega}}}{\rightleftarrows}}\; \text{skew symmetric } \boldsymbol{\Omega} \;\underset{\mathbf{w}=\mathbf{axial}(\boldsymbol{\Omega})}{\overset{\boldsymbol{\Omega}=\mathbf{spin}(\mathbf{w})}{\rightleftarrows}}\; \text{vector } \mathbf{w}$$

    with:

$$\mathbf{Q} = e^{\boldsymbol{\Omega}} = \mathbf{I} + \frac{\sin w}{w}\boldsymbol{\Omega} + \frac{\mathbf{1}-\cos^2 w}{w^2}\boldsymbol{\Omega}^2; \qquad w = \|\mathbf{w}\|$$

  - ⋆ no additive update, use products of rotation tensors:

$$\mathbf{R}^{n+1} = \Delta\mathbf{R}\mathbf{R}^{n}$$

- consistent linearization of all force terms

2.2 Activation of large deformations option in Z_SOIL code

The geometrical nonlinearity option is activated by the check box *Large displacement / rotations* in the bottom part of the dialog box *Analysis and drivers* under menu *Control / Analysis & Drivers*. The check box is active only if the version type is set as *Advanced* during *Control /Project preselection* or in the *Analysis and drivers* dialog.

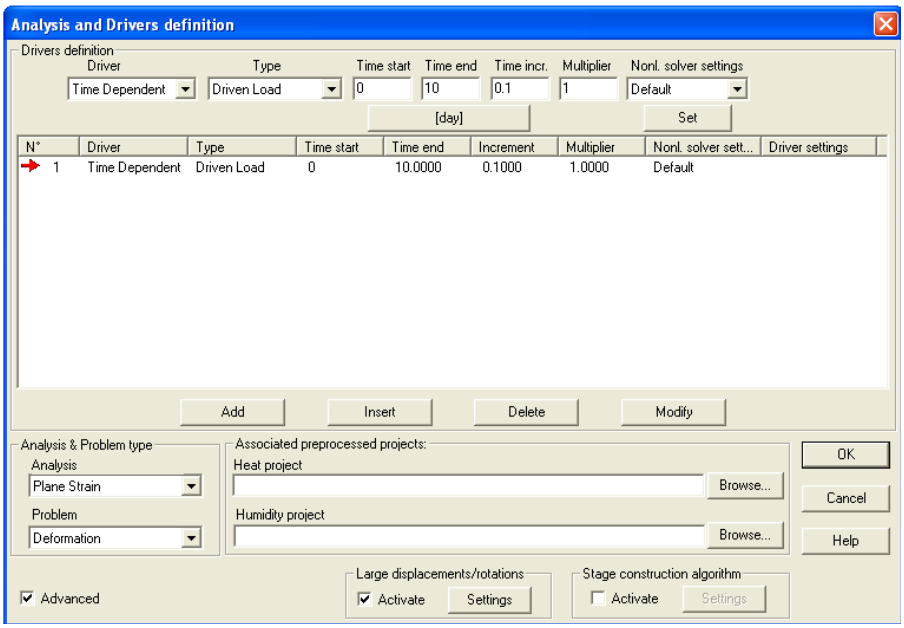

Figure 2.2: Analysis & Drivers dialog box

Remarks:

- once this option is activated the whole analysis will be run as geometrically nonlinear
- standard contact elements (segment to segment) cannot be used, only large deformation contact is allowed
- switching ON/OFF this option during restarts will yield computation failure

2.3 Benchmarks for beam elements

2.3.1 Euler problem (beam 2D). Eccentric compression in post-buckling range

Data file: Euler2D.inp

The problem of buckling of an elastic beam and tracing its behavior in the post-critical domain (reference: Życzkowski), is analyzed. The geometry, cross section and boundary conditions are shown in figure below. The uniform finite element mesh consisting of 10 equal size beam elements was used in the simulation. Material properties are as follows: $E = 100000$ [kPa], $\nu = 0.0$. This test is run as force driven starting from $N = 0$, $M = 0$ up to 4 times value of the Euler critical force ($N_{crit} = \frac{\pi^2 EJ}{(2L)^2} = 2.056$ [kN]) by gradually applying normal force and the moment. The comparizon of the reference solution by Życzkowski) and the numerical one is shown in the second figure.

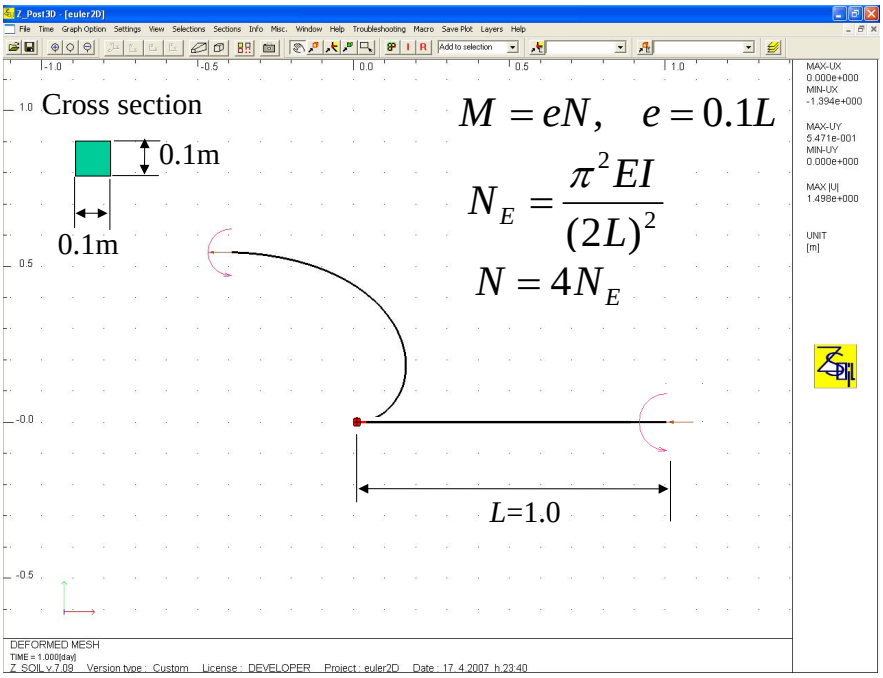

Figure 2.3: Euler beam problem. Data, initial and final configurations

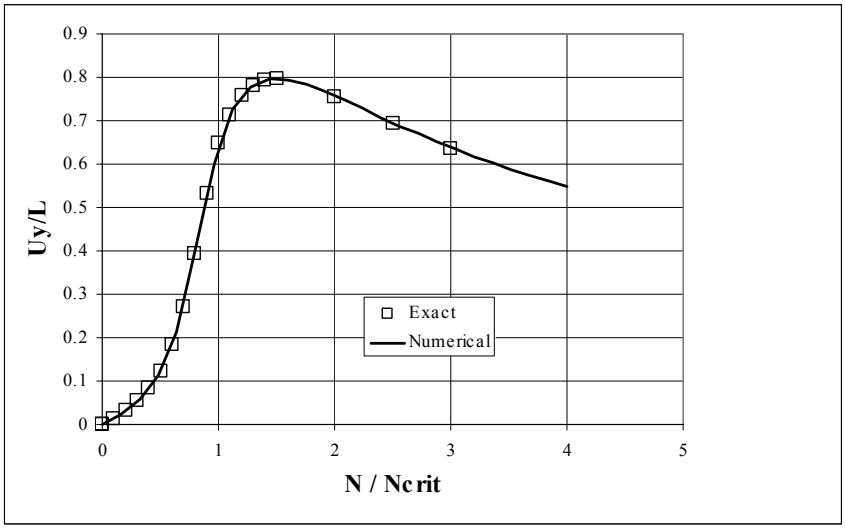

Figure 2.4: Euler problem. Force-displacement diagram

2.3.2 Curved 3D beam

Data file: Litewka-Wriggers.inp

The 3D problem of bending of an arch (see figure below) caused by the nodal force $F = 7\frac{EI}{R^2} = 2916.7$ [lbf] is analyzed. Geometry, cross section, boundary conditions and the load are shown in the figure below. Material properties are as follows: $E = 5.10^7$ [lbf/in2], $\nu = 0.2$

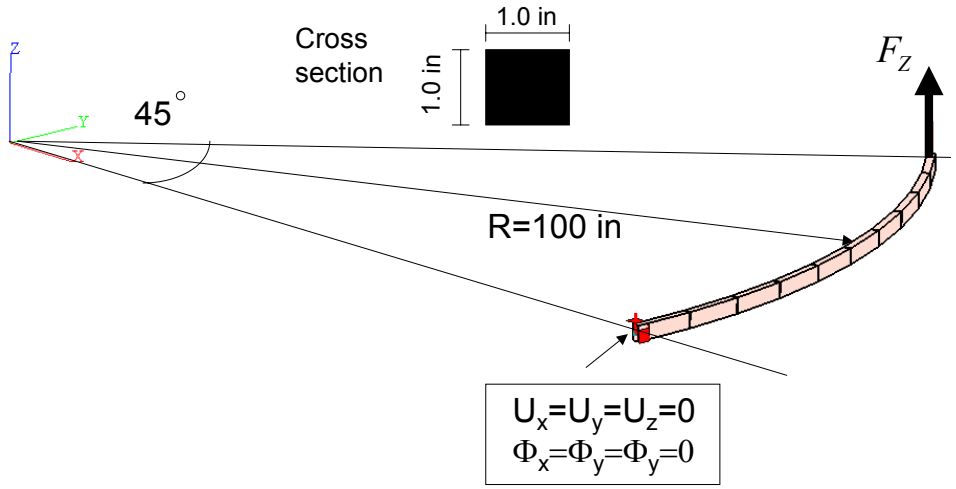

Figure 2.5: 3D Curved beam problem. Geometry, boundary conditions and mesh

The comparizon of the reference (Litewka, Wriggers) and numerical results for displacement vector at the point of application of the force is given in the table below.

	U[in] ref.solution	U[in] Z_SOIL result
U_x	13.5	13.5
U_y	-23.6	-23.6
U_z	54.0	53.3

2.4 Benchmarks for shell elements

2.4.1 Cylindrical shell under point forces.

Data file: Cylinder_free_edgeDC.inp

A cylindrical shell, shown in figure below, loaded by an imposed displacement is analyzed. Mesh, boundary conditions, material and geometrical parameters are also given in the figure. The comparizon of force-displacement diagram with the reference solution (Chróścielewski) is given in the next figure.

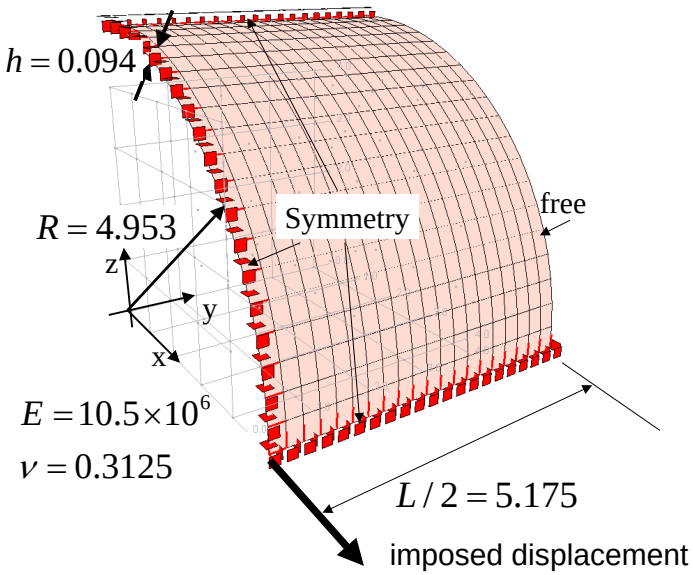

Figure 2.6: Free edge cylinder. The data

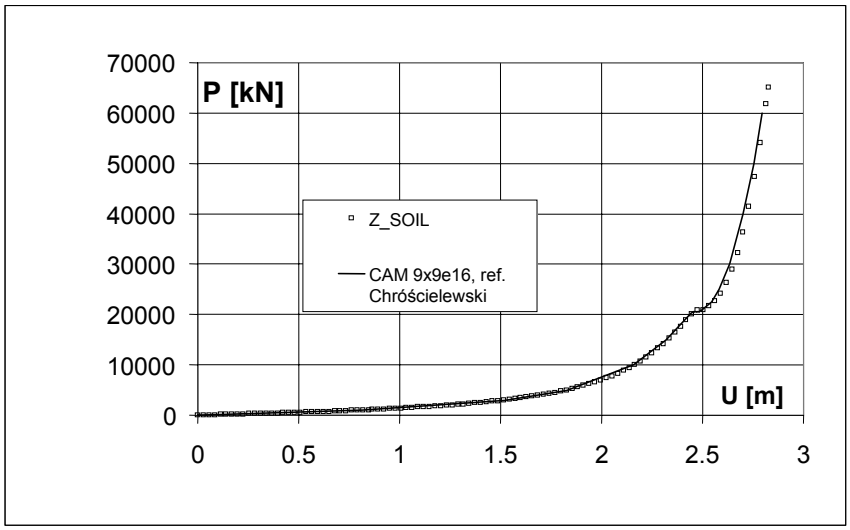

Figure 2.7: Free edge cylinder. Displacement history

2.4.2 Spherical shell under point force. Displacement control (post-buckling)

Data file: HingedSphereOnSquare.inp

A spherical shell, shown in figure below, loaded by an imposed displacement applied at the node at the origin of coordinate system is taken into consideration. Geometry of the shell, mesh and boundary conditions are shown in the figure. The comparizon of force-displacement diagram, at the node of application of the imposed displacement, versus reference solution after Chróścielewski is given in the next figure.

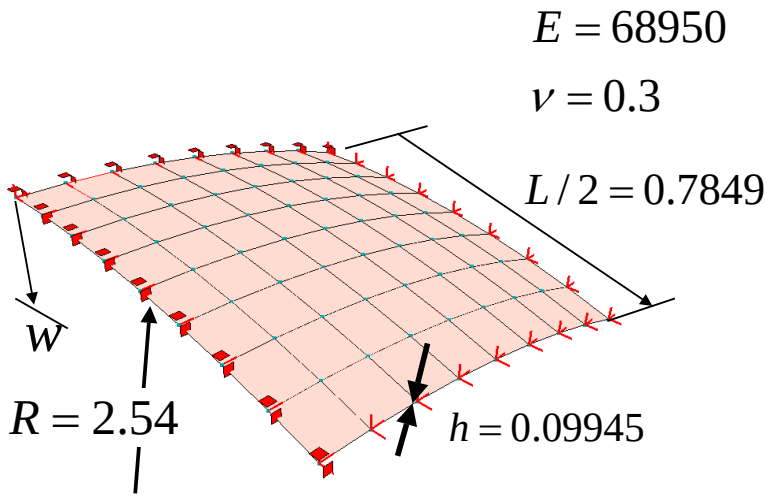

Figure 2.8: Clamped spherical shell. The data

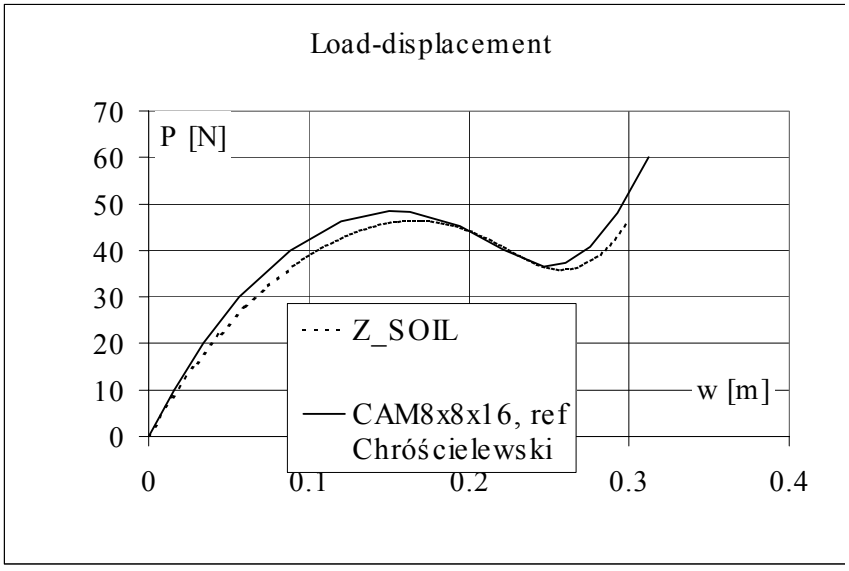

Figure 2.9: Clamped spherical shell. Load-displacement graph

2.5 Benchmarks for continuum elements

2.5.1 Euler problem in 2D

Data file: Euler-2d-continuum.inp

The problem of elastic buckling is analyzed here using exclusively continuum elements in the plane-strain format. The material imperfection is assumed by decreasing the E modulus in a single element shown in the figure. Geometry (L=10m, H=1m), mesh and boundary conditions are shown in figure below. The loading programme is driven by an imposed horizontal displacement applied to the point fixed at the right end of the beam. Material properties are as follows: $E = 100000$ kPa, $\nu = 0.0$. The theoretical buckling force according to the beam theory is equal to $F_{crit} = \dfrac{\pi^2 \, E \, J}{(2 \, L)^2}$ which yields $F_{crit} = 205.6$ kN/m. The force-deflection diagram is shown in the next figure.

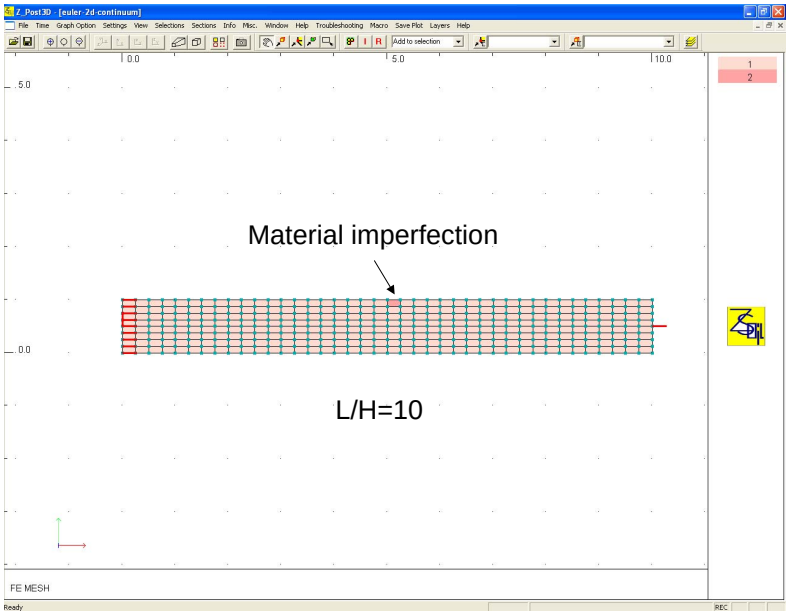

Figure 2.10: Elastic buckling problem in 2D

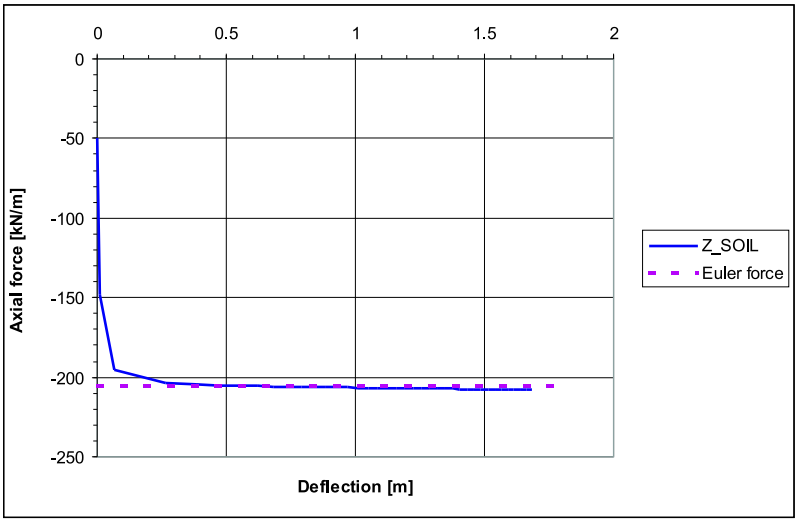

Figure 2.11: Force-deflection diagram

2.5.2 Euler problem in 3D

Data file: Euler-3d-continuum.inp

The problem of elastic buckling is analyzed here using exclusively continuum elements in the 3D format. The material imperfection is assumed by decreasing the E modulus in a single element shown in the figure. Geometry ($L = 10$ [m], $B = H = 1$ [m]), mesh and boundary conditions are shown in figure below. The loading programme is driven by an imposed horizontal displacement applied to the point fixed at the right end of the beam. Material properties are as follows: $E = 100000$ [kPa], $\nu = 0.0$. The theoretical buckling force according to the beam theory is equal to $F_{crit} = \dfrac{\pi^2 \, E \, J}{(2 \, L)^2}$ which yields $F_{crit} = 205.6$ kN/m. The force-deflection diagram is shown in the next figure.

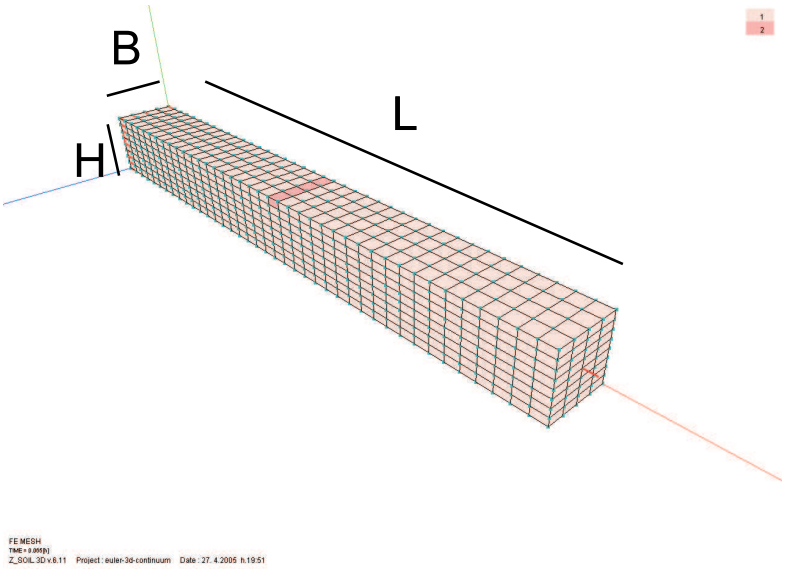

Figure 2.12: Elastic buckling problem in 3D

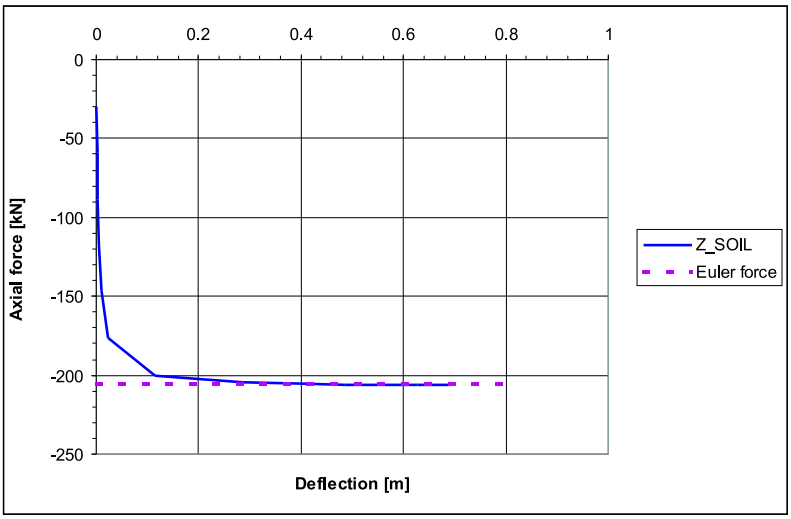

Figure 2.13: Force-deflection diagram

Chapter 3

Large deformation contact

3.1 Generation of large deformation interfaces

3.1.1 Setting slave-master attributes

In the ZSoil®2023code we use so-called node-segment elements. The contact interface in large deformations regime can be generated as continuum to continuum, continuum to shell, continuum to beam. So called symmetric contact should be generated always to avoid differences in results once switching between master and slaves is made. However, this is often not possible (beam interfaced with continuum 3D for instance) or not supported so far. All the possibilities in contact generation are given in the following 6 figures.

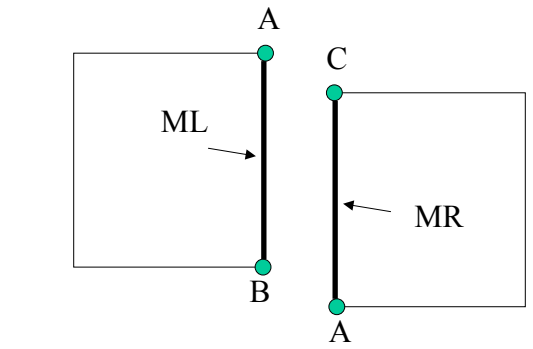

Slaves-L ={A,B}
Slaves-R={C,D}
Master-L={ML}
Master-R={MR}
Interface1 = { Slaves-L,Master-R}
Interface2 = { Slaves-R,Master-L}

Nonsymmetric contact: only Interface1 defined
or Interface2
Symmetric contact: both Interface1 and
Interface2 exist

Figure 3.1: Continuum 2D - Continuum 2D interface setting

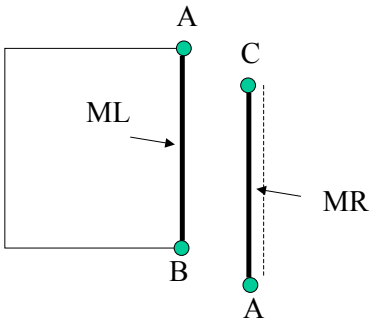

Slaves-L ={A,B}
Slaves-R={C,D}
Master-L={ML}
Master-R={MR}
Interface1 = { Slaves-L,Master-R}
Interface2 = { Slaves-R,Master-L}

Nonsymmetric contact: only Interface1 defined or Interface2
Symmetric contact: both Interface1 and Interface2 exist

Figure 3.2: Continuum 2D - Beam 2D interface setting (case 1)

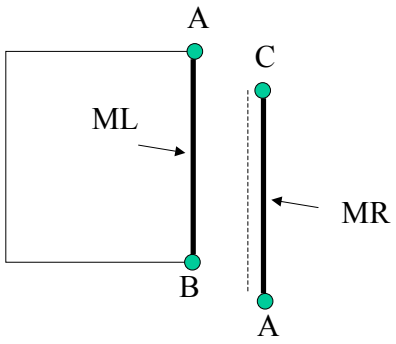

Slaves-R={C,D}
Master-L={ML}
Interface2 = { Slaves-R,Master-L}

Nonsymmetric contact: only Interface2 is possible

Figure 3.3: Continuum 2D - Beam 2D interface setting (case 2)

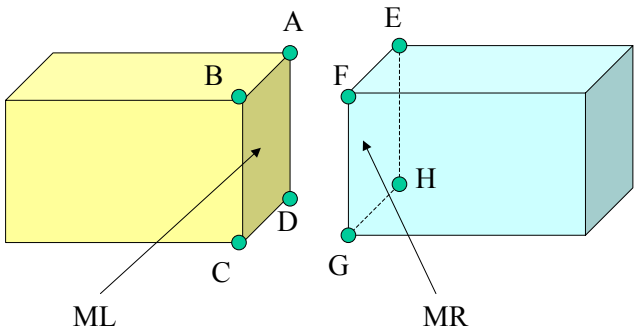

Slaves-L ={A,B,C,D}
Slaves-R={E,F,G,H}
Master-L={ML}
Master-R={MR}
Interface1 = { Slaves-L,Master-R}
Interface2 = { Slaves-R,Master-L}

Nonsymmetric contact: only Interface1 defined or Interface2
Symmetric contact: both Interface1 and Interface2 exist

Figure 3.4: Continuum 3D - Continuum 3D interface setting

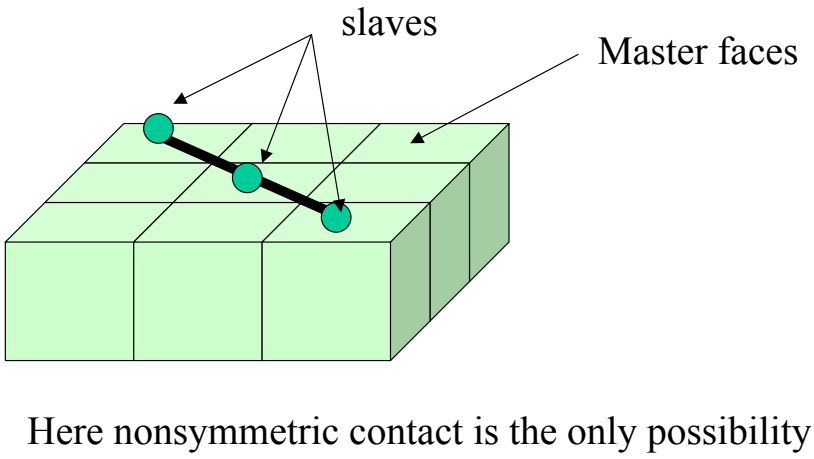

Figure 3.5: Continuum 3D - Beam3D interface setting

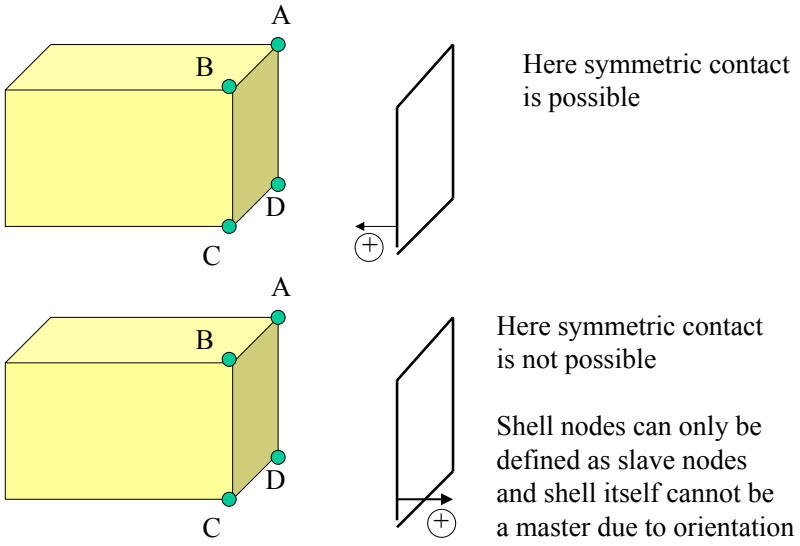

Figure 3.6: Continuum 3D - Shell interface setting

3.1.2 Generation of large deformation interfaces for evolving structures

The two general approaches concerning generation of contact interfaces (node-segment) for problems in which the geometry is varying in time are implemented in the current version. In the first approach deformations during construction must be small while in the second approach this restrictive assumption is no more valid. In the first approach new contact interface added in the subsequent fill step cancels the initial deformation of the contacting bodies (for instance lining and fill material) and this the reason why it can be used exclusively when initial deformations of the contacting bodies (during construction !) are small enough. In this approach all rules concerning slave-master setting, given in the previous section, are valid.

The second approach is more general but it yields some limitations on slave-master setting. To explain the general idea lets us consider an example of excavation followed by lining construction and then filling. The aim of the simulation is to to perform an excavation and then construction of a lining followed by seven stages of filling (see Fig. 3.7). After an excavation we get some deformations which we will neglect when a tunnel lining is built. To do that the program memorizes total deformation $\mathbf{U}_e$. This is done automatically (see Fig.3.8). In the next step the tunnel lining is added and its initial configuration is assumed to be undeformed (just before construction) regardless nonzero deformation at nodes at the bottom slab of the lining. This can be managed thanks to the memorized deformation $\mathbf{U}_\mathrm{e}$. The major problem appears when we begin to add fill material. This is so because newly added fill should satisfy contact kinematics if it touches already deformed lining (due to its own dead weight and/or loading imposed during previous fill steps)and existing deformation on the remaining boundaries (see Fig.3.9). If we consider the situation shown in Fig.3.10 we can notice that the initial undeformed mesh in the zone of fill (stage I) must be mapped onto deformed configuration caused by a construction of a lining. Hence the boundary nodes along section A-B must satisfy the contact kinematics (cannot penetrate the lining and cannot be separated from it), nodes along the boundary A-D and D-E must fit current deformation equal to $\mathbf{U} - \mathbf{U}_e$ (the one corresponding to the settlement caused by lining construction), and nodes along section E-B must remain at the initial elevation.

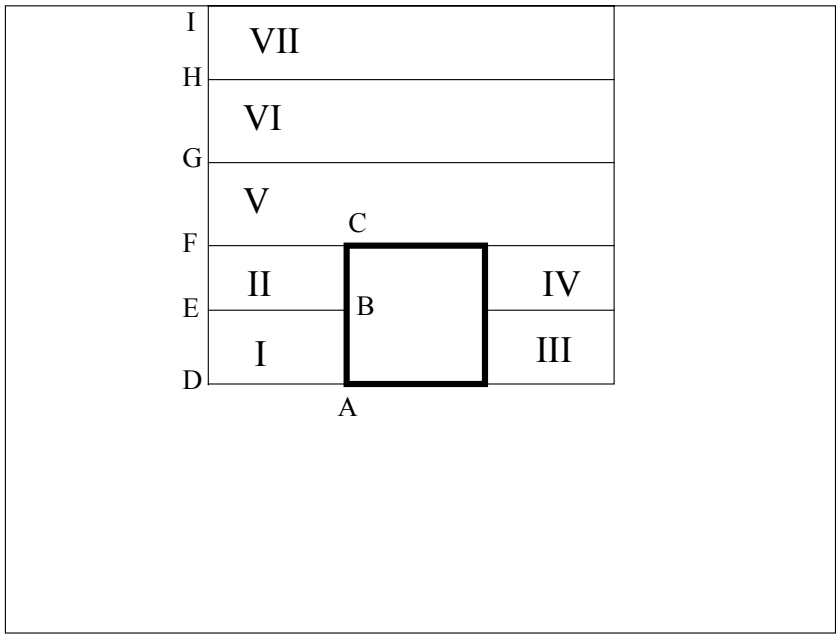

Figure 3.7: Tunnel construction followed by several fill steps

This mapping is made in the code by a finite element solution of a sub-domain subject to the imposed boundary displacements. As the result we get a shift to the nodal coordinates of all newly added continuum elements (NB. in this finite element sub-problem we assume artificial elastic constants $E = 1.0$ and $\nu = 0.0$). However, to make this mapping, all nodes along the section A-B, being part of the contact interface, **must be slave nodes (!)**. It should be emphasized here that incremental deformations during single fill step should be small otherwise strain incompatibilities along the section A-D can cause stress oscillations (although total deformation caused by filling can be large).

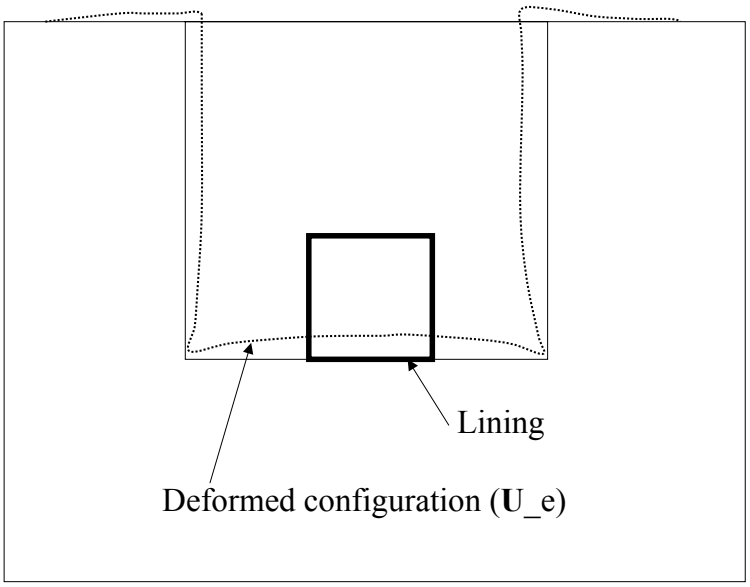

Figure 3.8: Registering total deformation after excavation

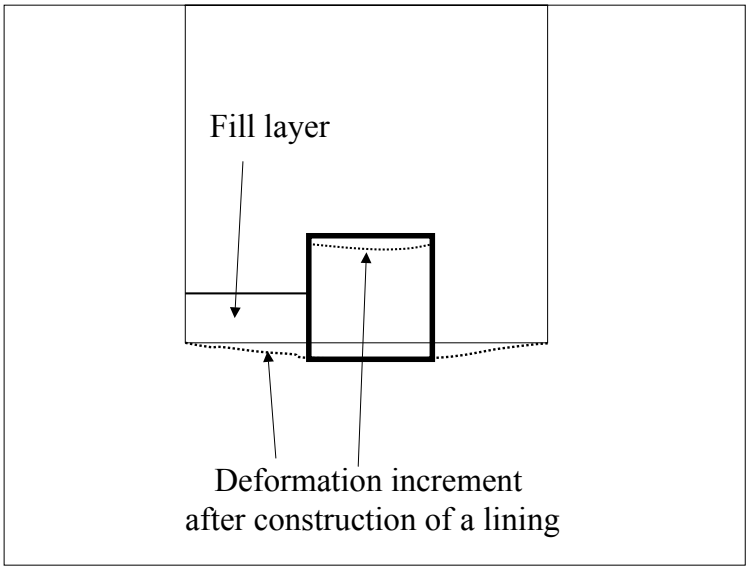

Figure 3.9: Deformation increment due to construction of the lining

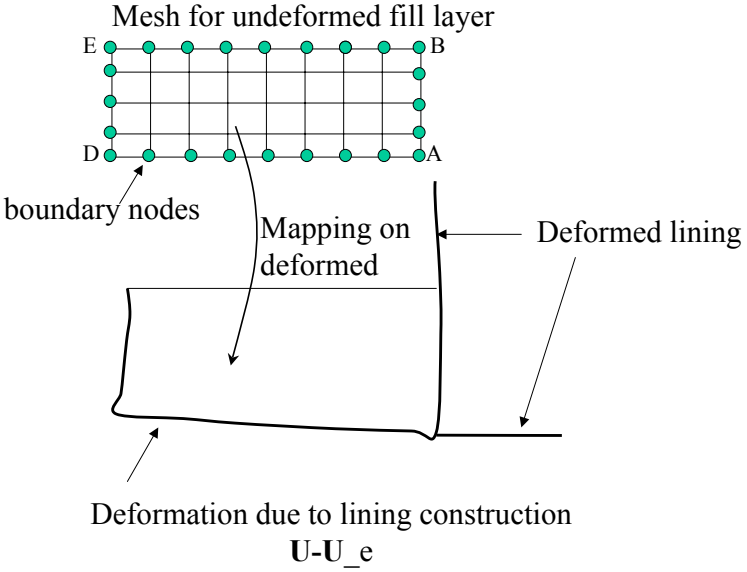

Figure 3.10: Mapping of the fill subdomain onto deformed configuration

To summarize the following general rules are used in the second approach:

- structures (beams/truss/membranes/shells) are always added in undeformed configuration; hence, whenever new structural element is added its initial total deformation must be memorized as Uo_s (at the element level); the current structure deformation is always equal to $\mathbf{U} - \mathbf{U}_{os}$
- continuum is added after mapping to the deformed configuration
- at the end of the excavation time step the current total deformation corresponding to that state is memorized as $\mathbf{U}_e$ for all nodal points

Mapping from undeformed to the deformed configuration is performed by imposing displacements at the boundary nodes according to the following rules:

- if node is of SLAVE type then we project it on master in the following manner
  if master is a structural element then impose on slave node a shift equal to $\mathbf{U} - \mathbf{U}_{os}$
  if master is not a structural element impose on slave node a shift equal to $\mathbf{U} - \mathbf{U}_e$

- if node is not of a SLAVE type then
  if node belongs to the structural element existing at time t_N then set shift $\mathbf{U} - \mathbf{U}_{os}$
  if node does not belong to the structural element existing at time t_N then set shift $\mathbf{U} - \mathbf{U}_e$

- if node has a solid BC on certain DOF then impose them
- if node is on the free external boundary impose zero deformation in y direction

NB. Activation of the approach II has be done in the dialog *Control /Analysis and drivers* by switching the *Large displacement /rotations* ON. Then under *Settings*, in the appearing dialog checkbox *Update coordinates during costruction* has to be set ON, otherwise algorithm I will be performed

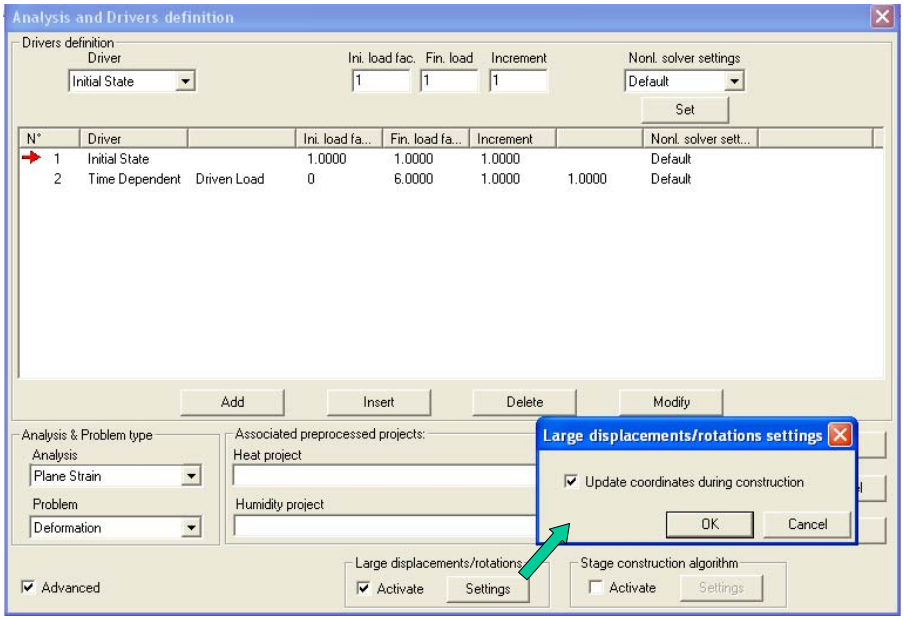

Figure 3.11: Activating algorithm II

3.1.3 Example for generation of contact interfaces in 2D large deformation application - approach I

Data file: test-frame-filling.inp

Let us consider an example of an excavation and then tunnel construction followed by filling. The main problem is on how to generate contact interface starting with mesh as shown in Fig.(3.12). To do that we have to disconnect the mesh along the interface contour. In this example all nodes which belong to the continuum elements adjacent to the lining and being external to the lining have new node numbers. This operation can be performed in the following manner:

1. select all quads inside lining
2. select all beams (see Fig.(3.13)
3. remove selected elements virtually (hide them)
4. select nodes to be duplicated (see Fig.(3.14)
5. under menu *Interfaca(large deformation)* use method *Create new nodes on selected..*
   at that moment we have duplicated nodes along the lining and new nodes belong to the continuum elements adjacent to beams (see Fig.(3.15)

Once we have disconnected the mesh along the contour we can generate contact interface in the following way

1. highlight contact element contour (edges which will play a role of so-called masters) (see Fig.(3.16), and create masters with a label "masters"
2. select part of the lining (beam elements) (see Fig.(3.17)and then select nodes from selected beam elements
3. create group of slave nodes (contactors) with a label "slave nodes on beam"
4. using an option *Create\Update contact elements* define the interface by merging the pair "slave nodes on beam"-"masters" (see Fig.(3.18, Fig.(3.19)

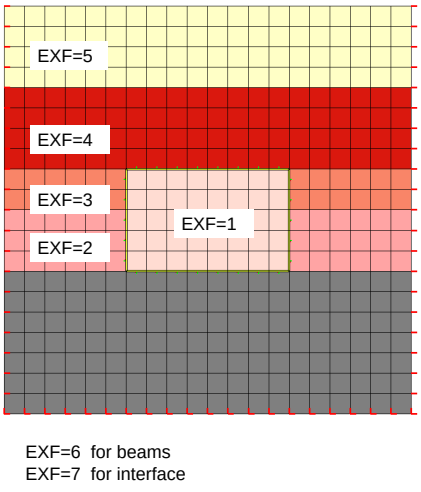

Figure 3.12: Mesh and distribution of existence functions

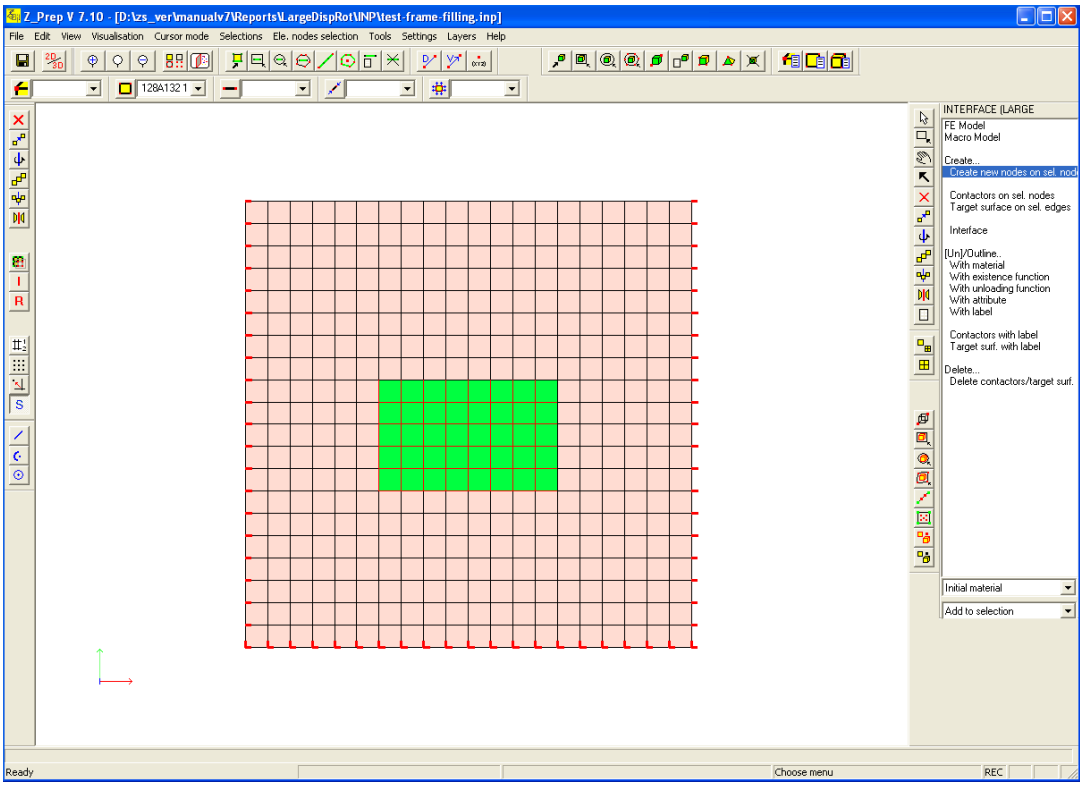

Figure 3.13: Selection of the lining interior

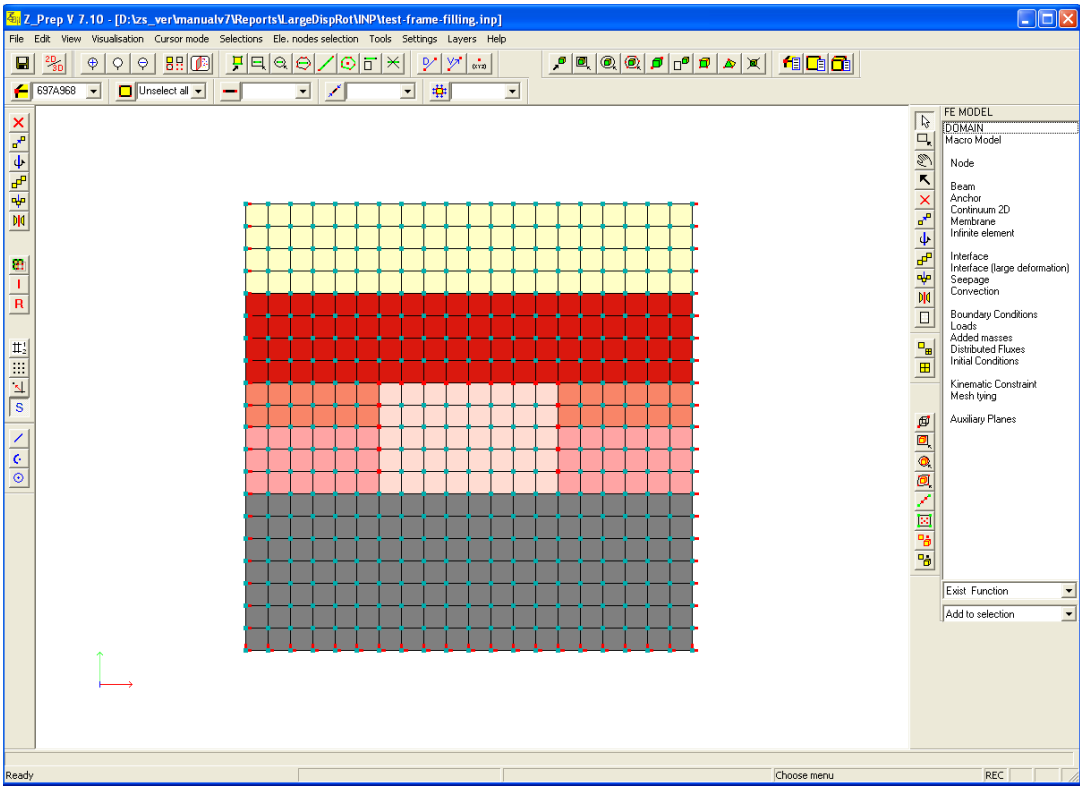

Figure 3.14: Selection of nodes to be duplicated

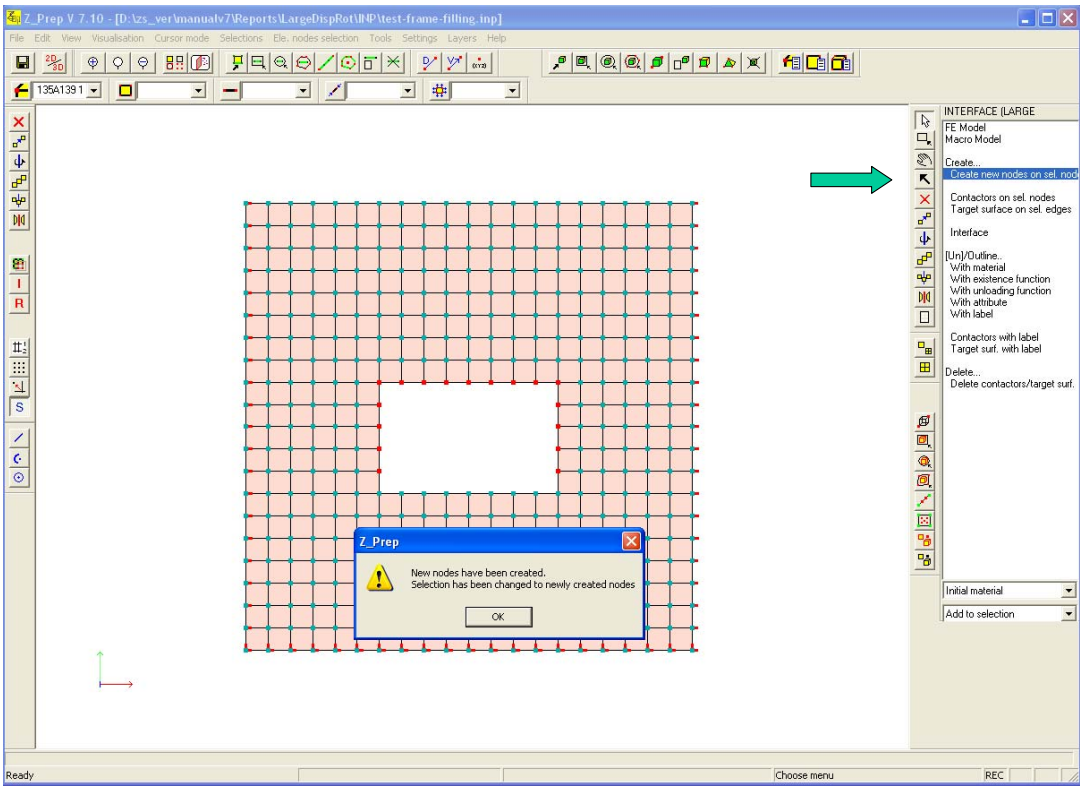

Figure 3.15: Nodes after duplication procedure

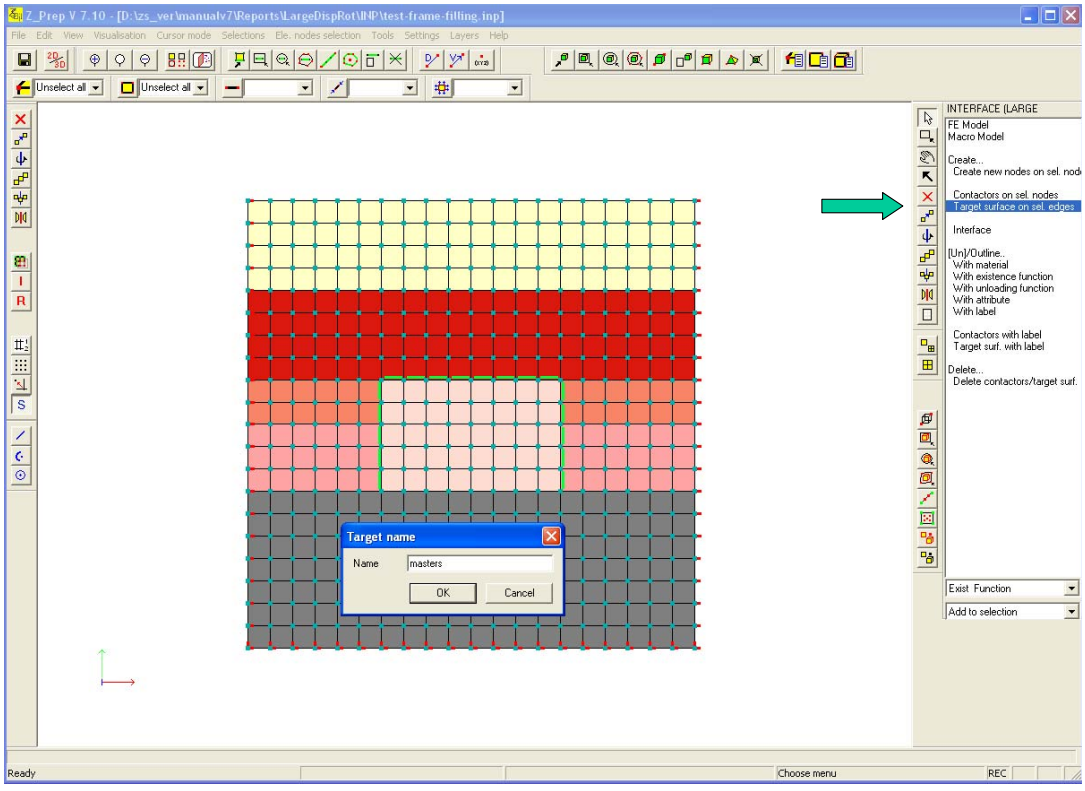

Figure 3.16: Generation of masters

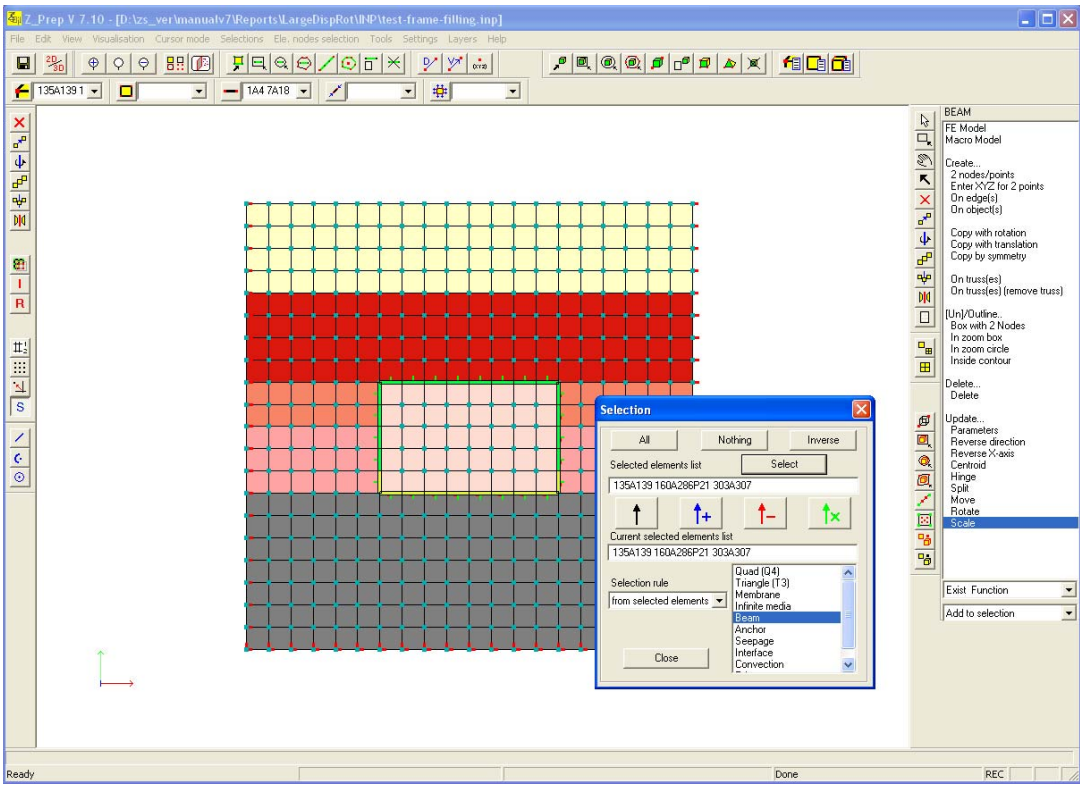

Figure 3.17: Selection of nodes to set them as slaves

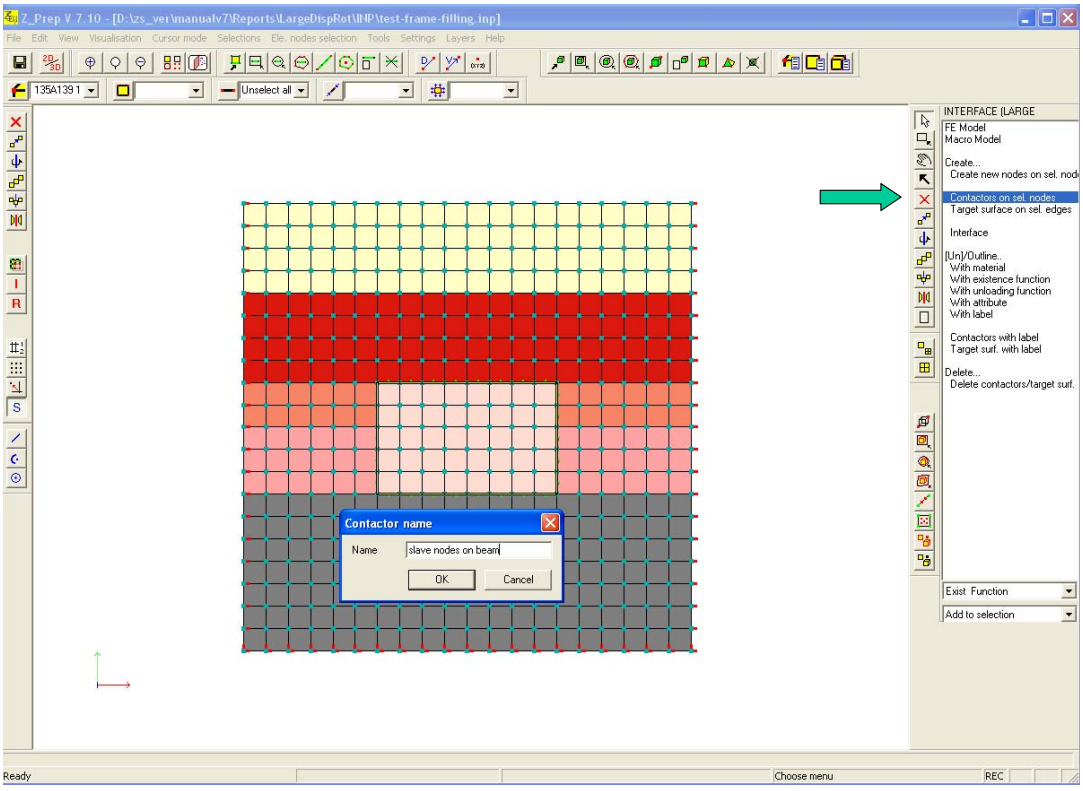

Figure 3.18: Generation of slave nodes

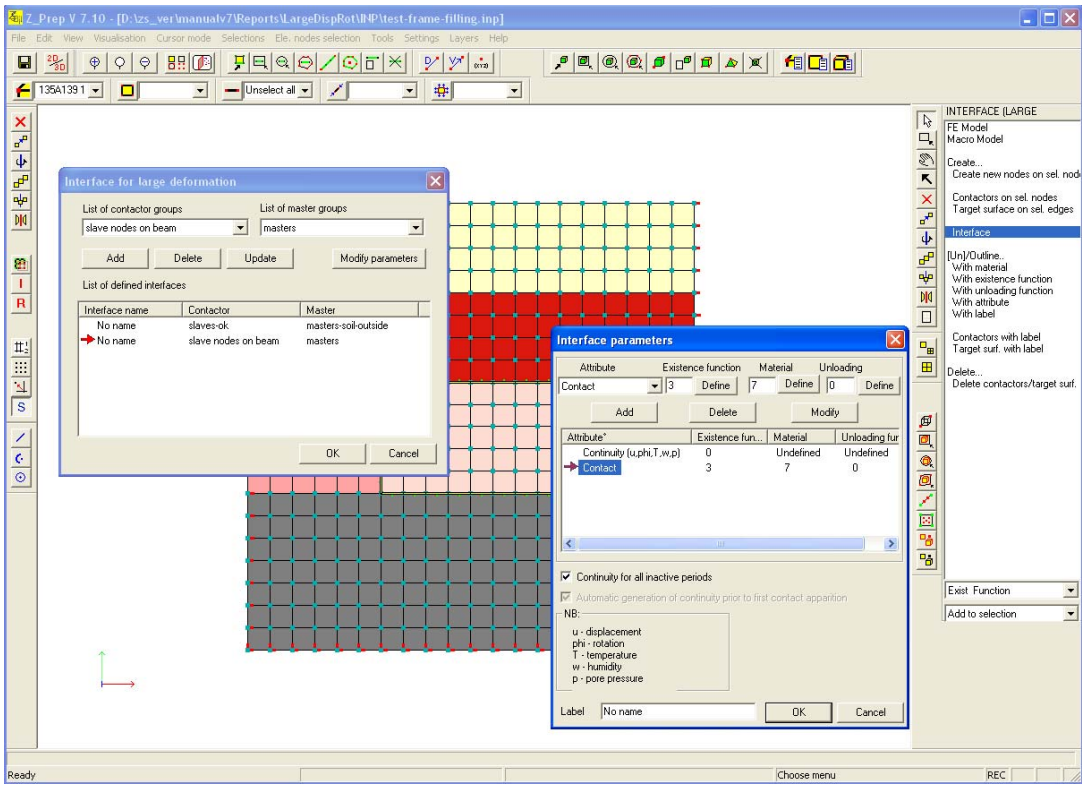

Figure 3.19: Definition of contact interface

3.1.4 Example for generation of contact interfaces in 2D large deformation application - approach II

Data file: test-frame-filling-n.inp

The same example analyzed with the second approach requires a different setting for the interface. The details of the data generation are given in the following 5 figures.

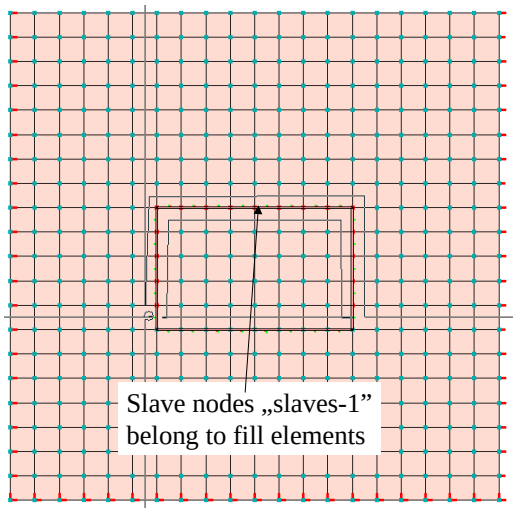

Figure 3.20: Slave nodes location

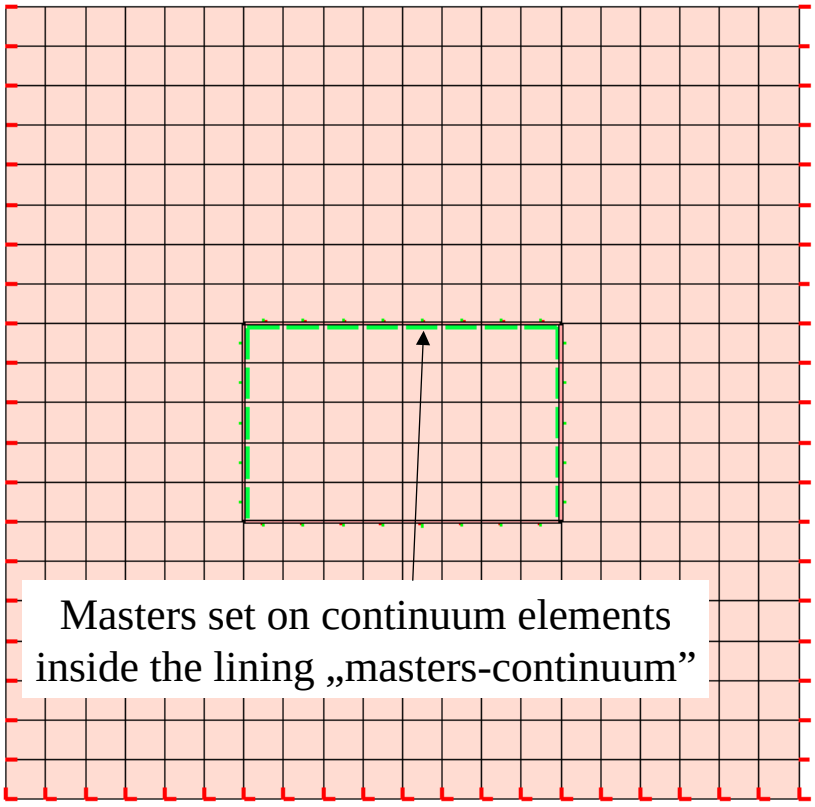

Figure 3.21: Location of masters to handle continuity condition before excavation

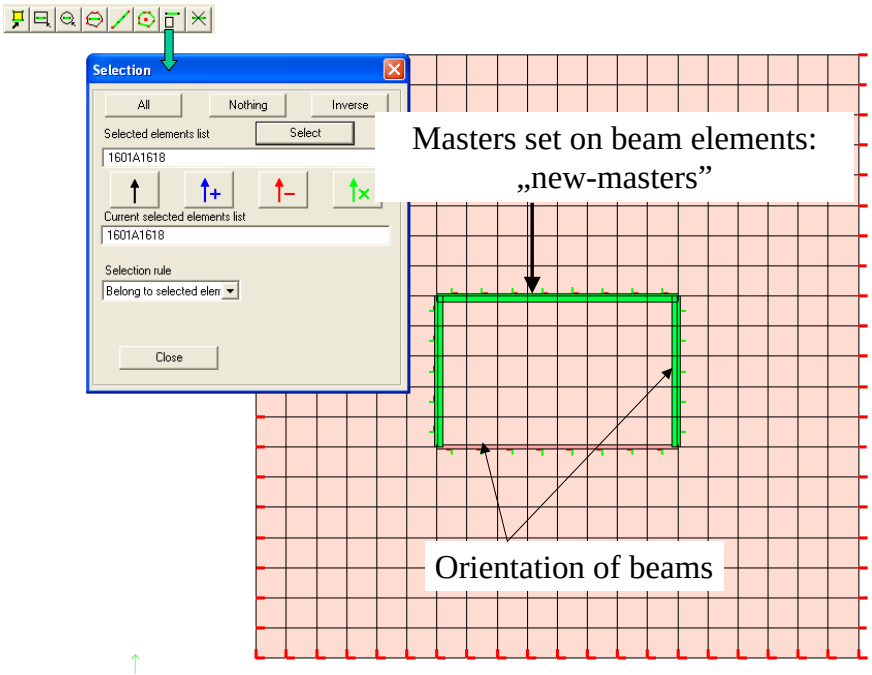

Figure 3.22: Location of masters to handle filling

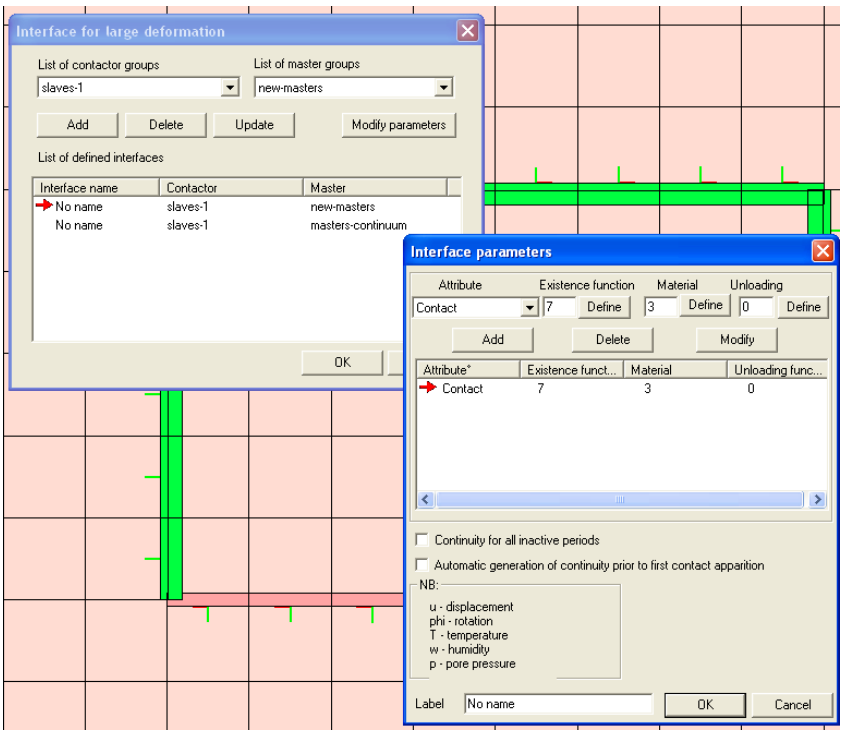

Figure 3.23: Setting contact interface parameters for interface structure-fill

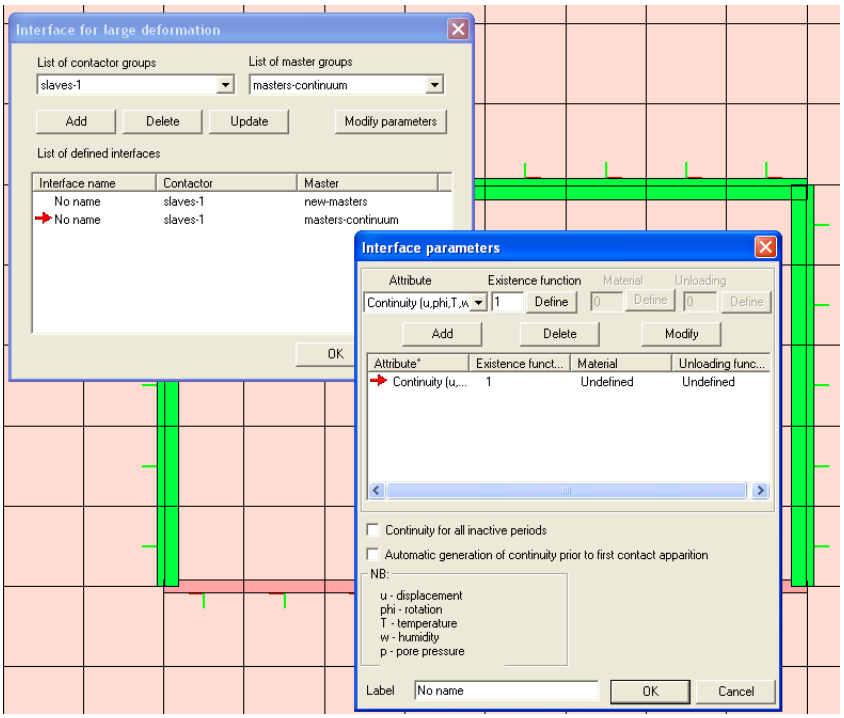

Figure 3.24: Setting continuity interface along initial position of the lining contour

3.2 Benchmarks for contact interfaces

Data preparation in this case is somewhat different compared to the standard contact interface setting known for small deformation applications. In the large deformations regime slave nodes may interact with different master faces during the analysis hence explicit setting of so-called contact elements is not possible. In general we may associate the attribute "contactor node" with any node in the mesh and another attribute which is the "master face" with any face of the finite element (continuum, shell, beam (only 2D) or membrane).

3.2.1 Hertz problem

Data files : hertz-2d-dense-foundation, hertz-2d

The classical Hertz problem in the plane-strain format is analyzed in this section. The reference solution was taken from paper by Papadopoulos and Taylor (P. Papadopoulos and R. L. Taylor. A mixed formulation for the finite element solution of contact problems. Computer Methods in Applied Mechanics and Engineering 94 (1992) p. 373-389).

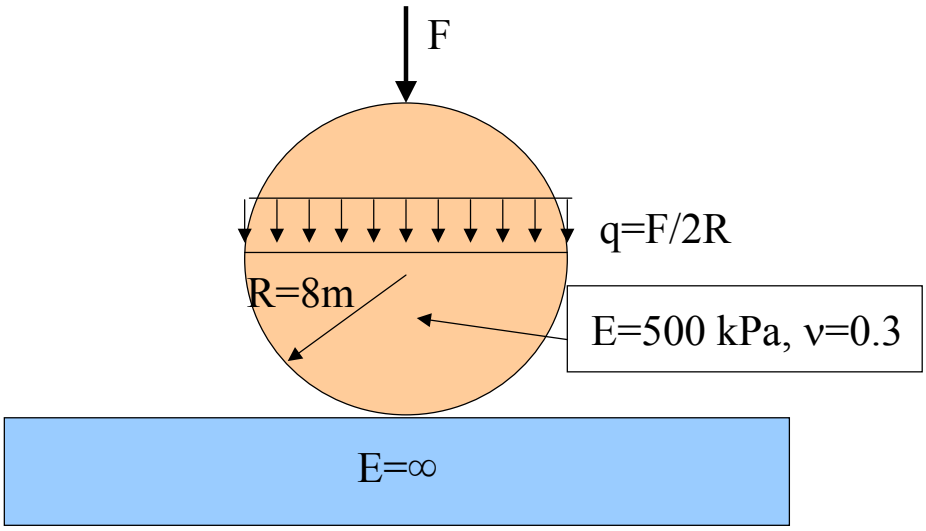

Figure 3.25: Hertz problem setting

As the foundation is to be rigid we can generate the mesh as shown in figure 3.26. However, contact stress recovery is not that easy matter in the node-segment contact implementations. Hence we can generate different mesh for the foundation with which, using standard tools available in the postprocessor (cross sections through the mesh), we can easily recover the interesting values. This second mesh is shown in figure 3.27.

The comparison of normal stresses in the interface for two levels of the force $F = 50$ kN/m and $F = 100$ kN/m ($q = \frac{F}{2R}$) is presented in figure 3.28.

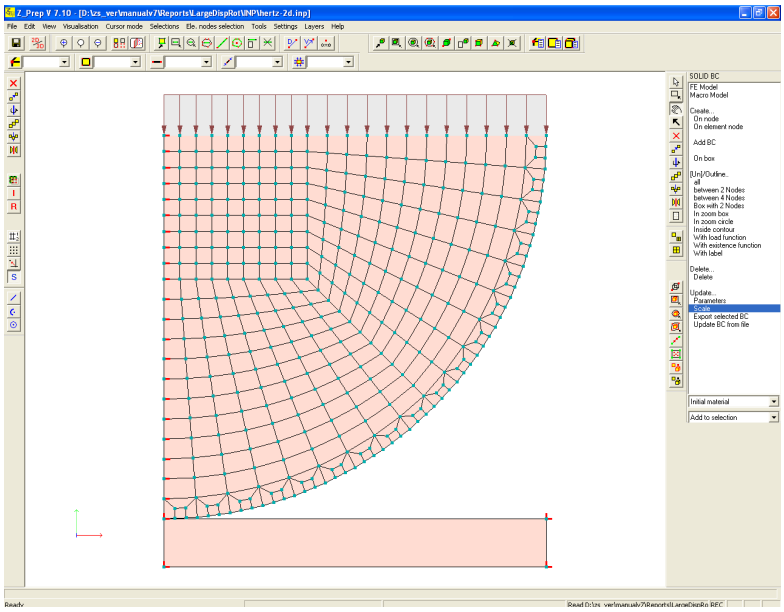

Figure 3.26: Hertz problem in plane strain format

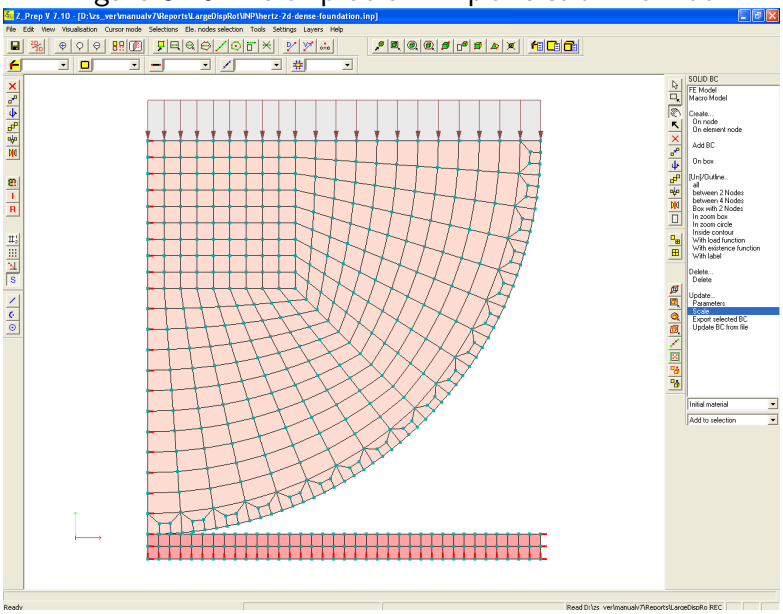

Figure 3.27: Hertz problem in plane strain format - dense mesh in the foundation

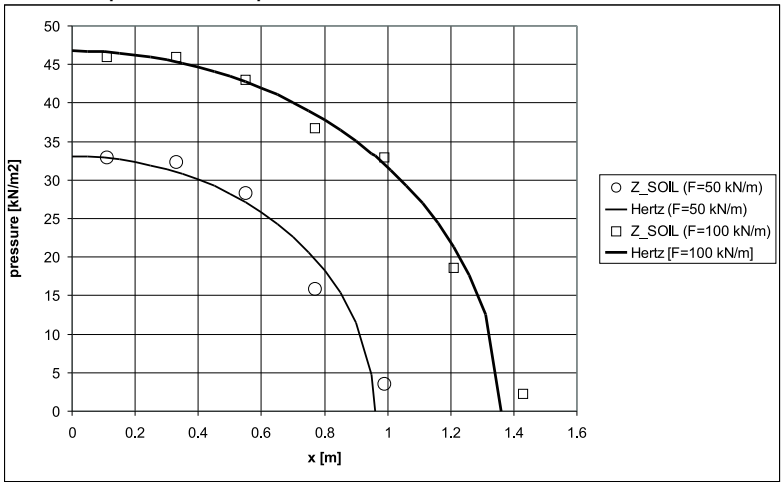

Figure 3.28: Hertz problem: Distribution of contact stresses

3.2.1.1 Generation of contact interfaces for Hertz problem

The following figures explain on how to create contact interfaces in the 2D applications.

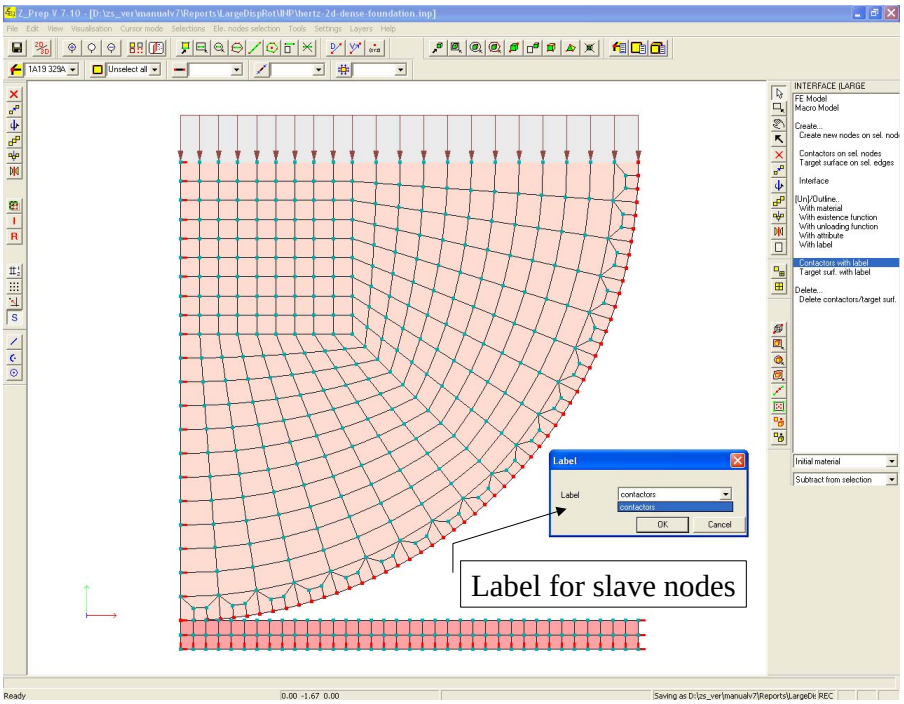

Figure 3.29: In menu *INTERFACE (LARGE DEFORMATIONS)* create group of slave nodes (contactors)

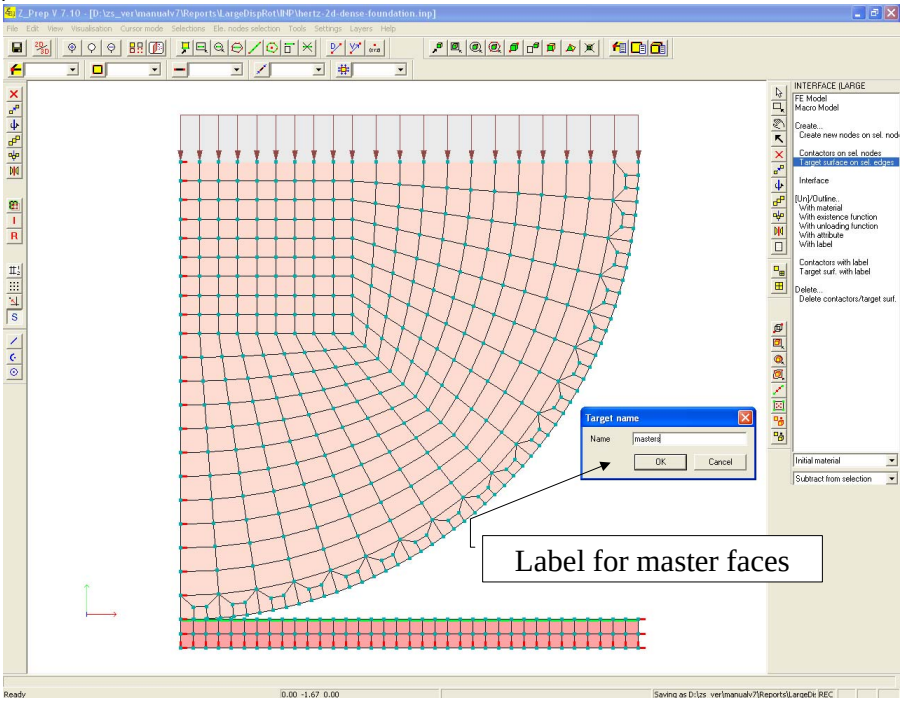

Figure 3.30: In menu *INTERFACE (LARGE DEFORMATIONS)* create group of master faces

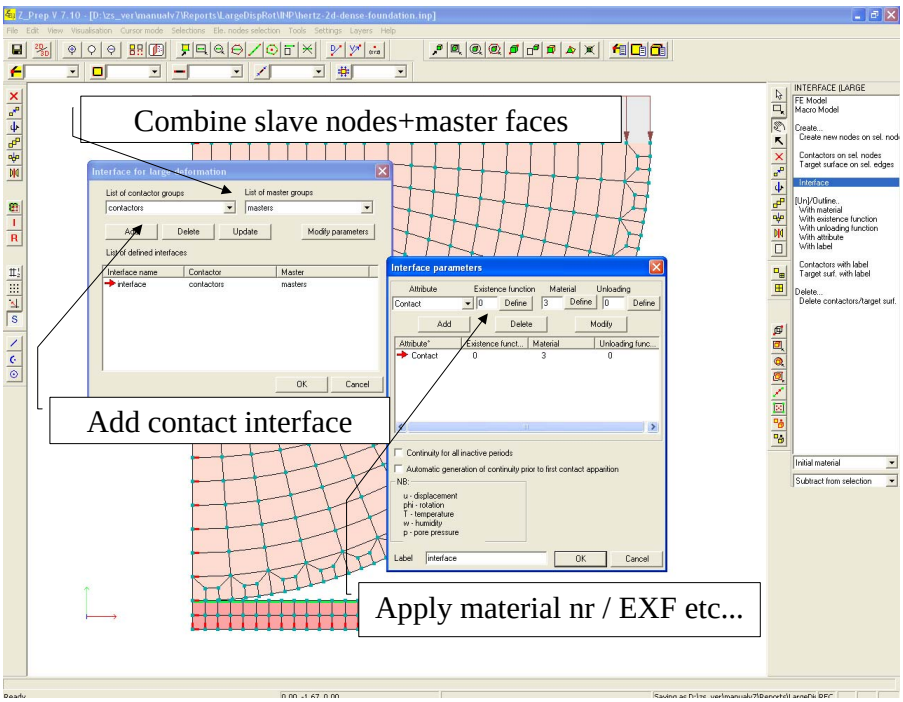

Figure 3.31: Definition of the interface for Hertz problem. In menu *INTERFACE (LARGE DEFORMATIONS)* select one group of slaves and one group of master faces and add to list of interfaces

3.2.2 Example of two contacting wheels

Data file: two-wheels.inp

The aim of this example is to show some details concerning generation of the large deformation contact interfaces. The important thing is that in cases of the two deformable bodies we should generate so-called symmetric contact in which boundaries of the two bodies have both slave nodes and master faces. This test is driven by applied vertical displacement.

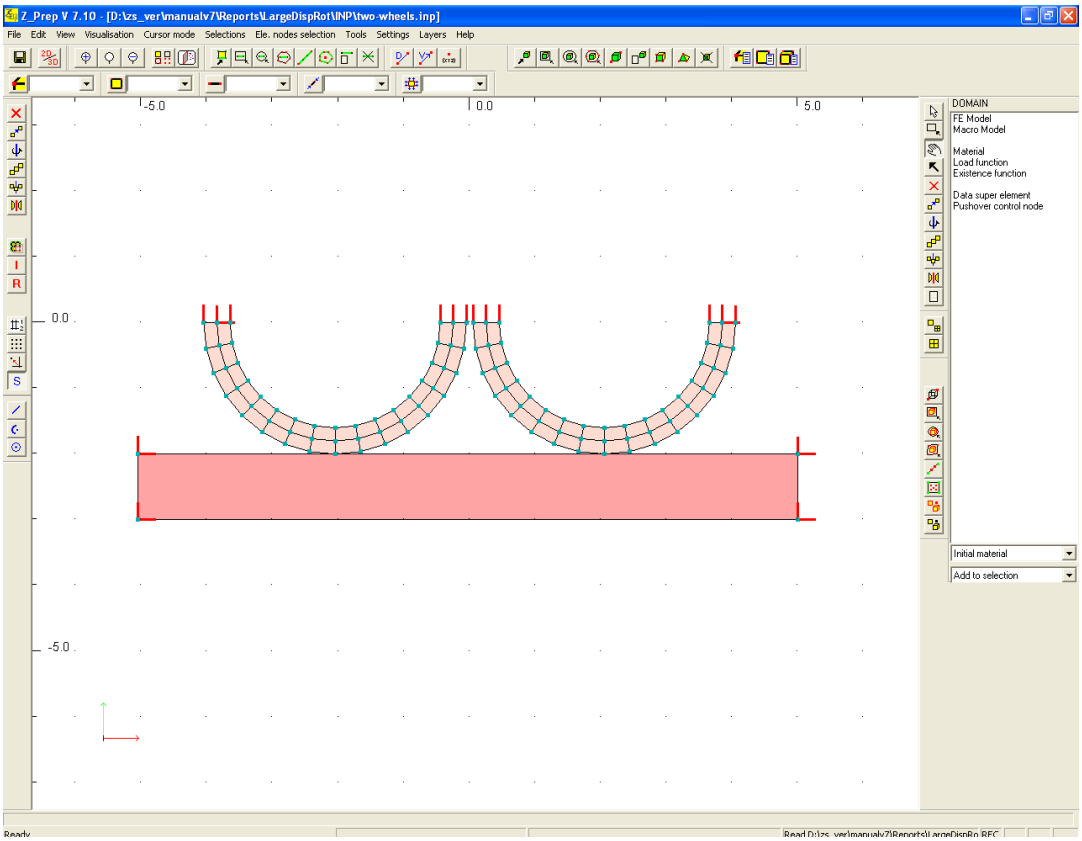

Figure 3.32: Finite element meshes for two wheels and foundation

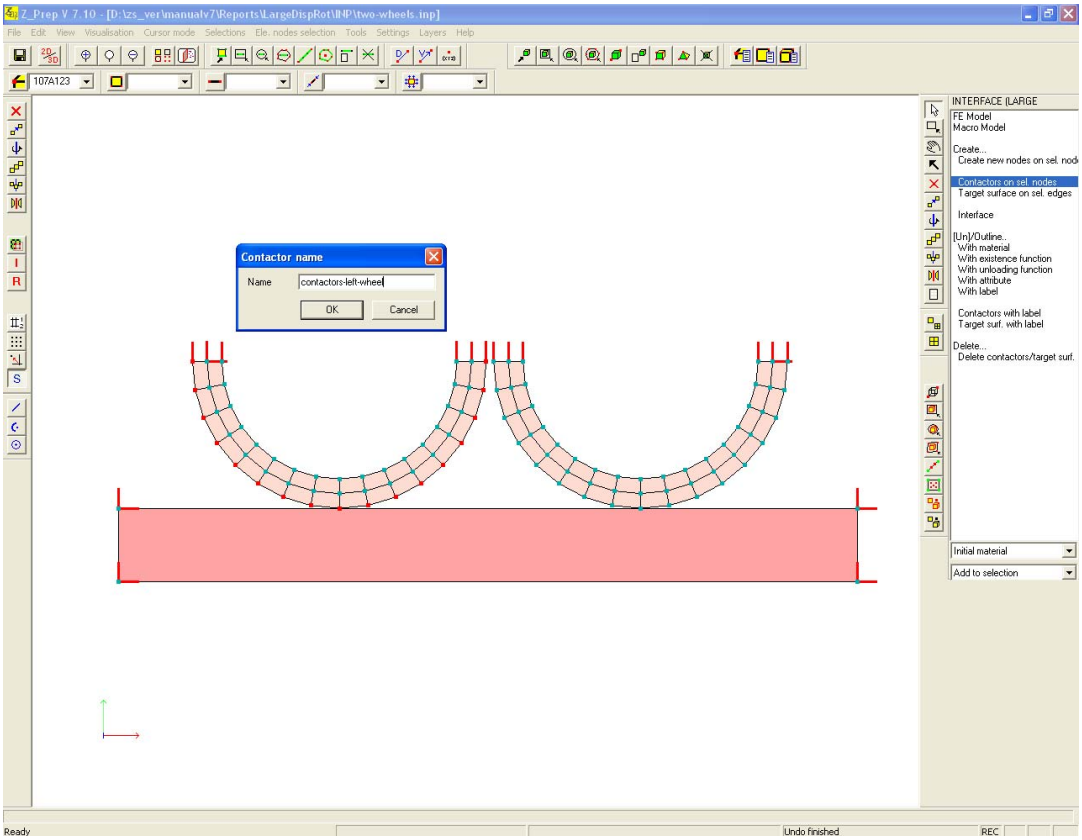

Figure 3.33: Setting slave nodes (contactors) on left wheel

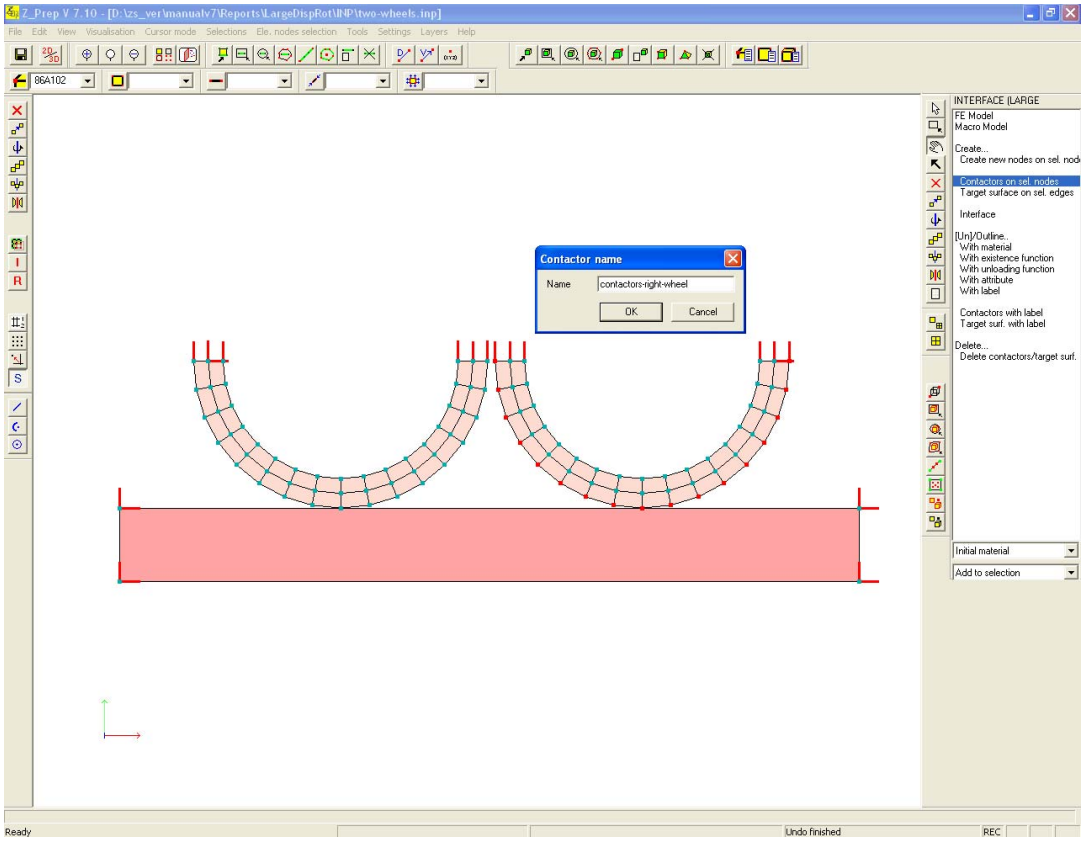

Figure 3.34: Setting slave nodes (contactors) on right wheel

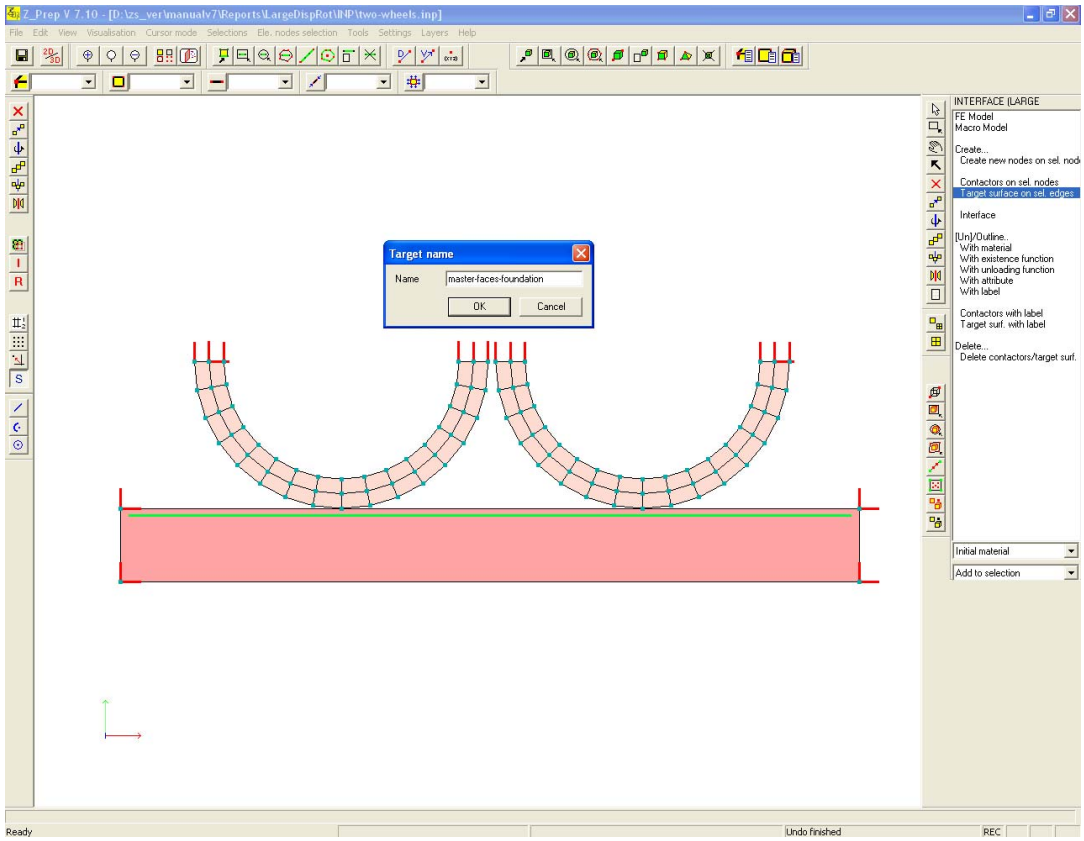

Figure 3.35: Setting master faces on foundation mesh

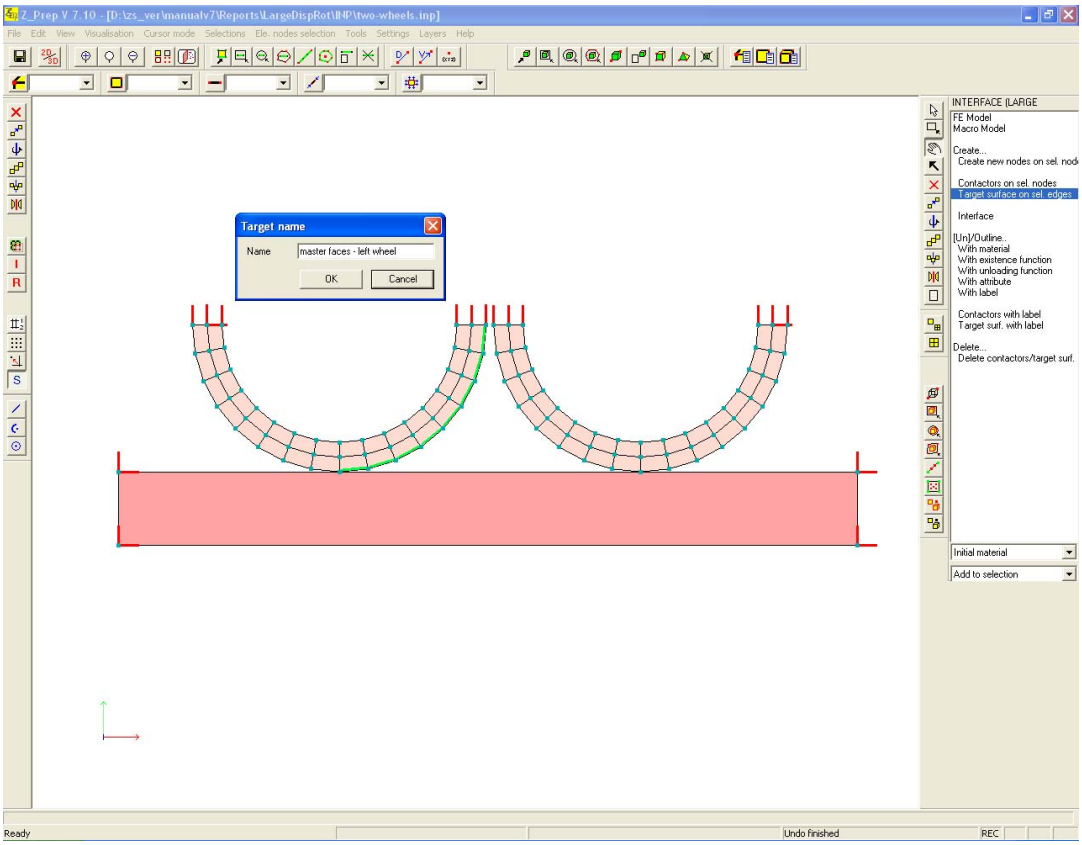

Figure 3.36: Setting master faces on left wheel

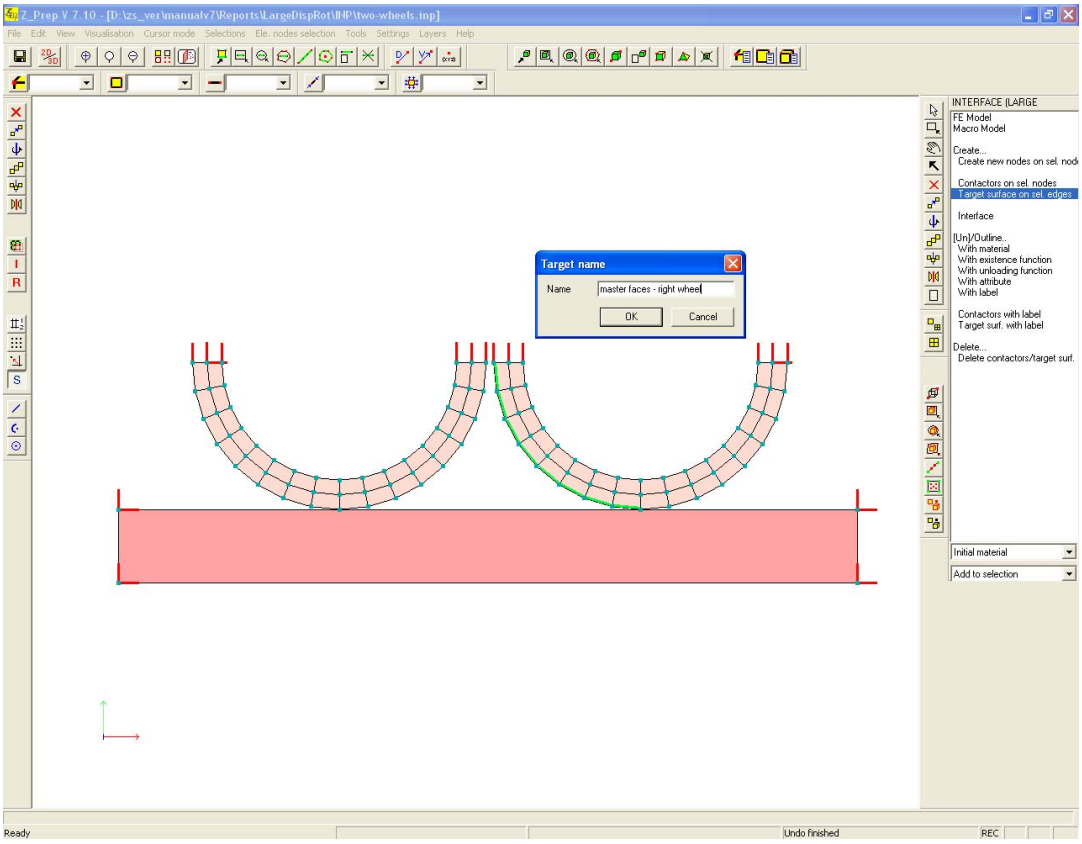

Figure 3.37: Setting master faces on right wheel

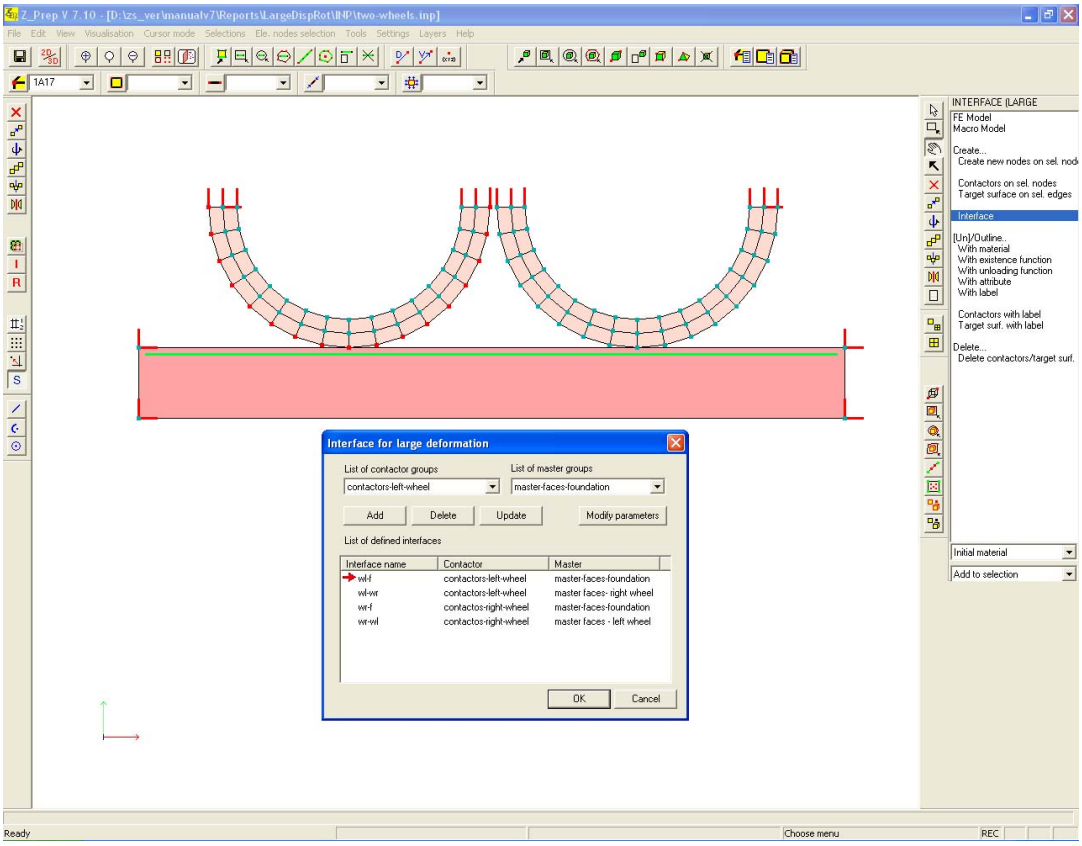

Figure 3.38: Generation of interface left wheel-foundation

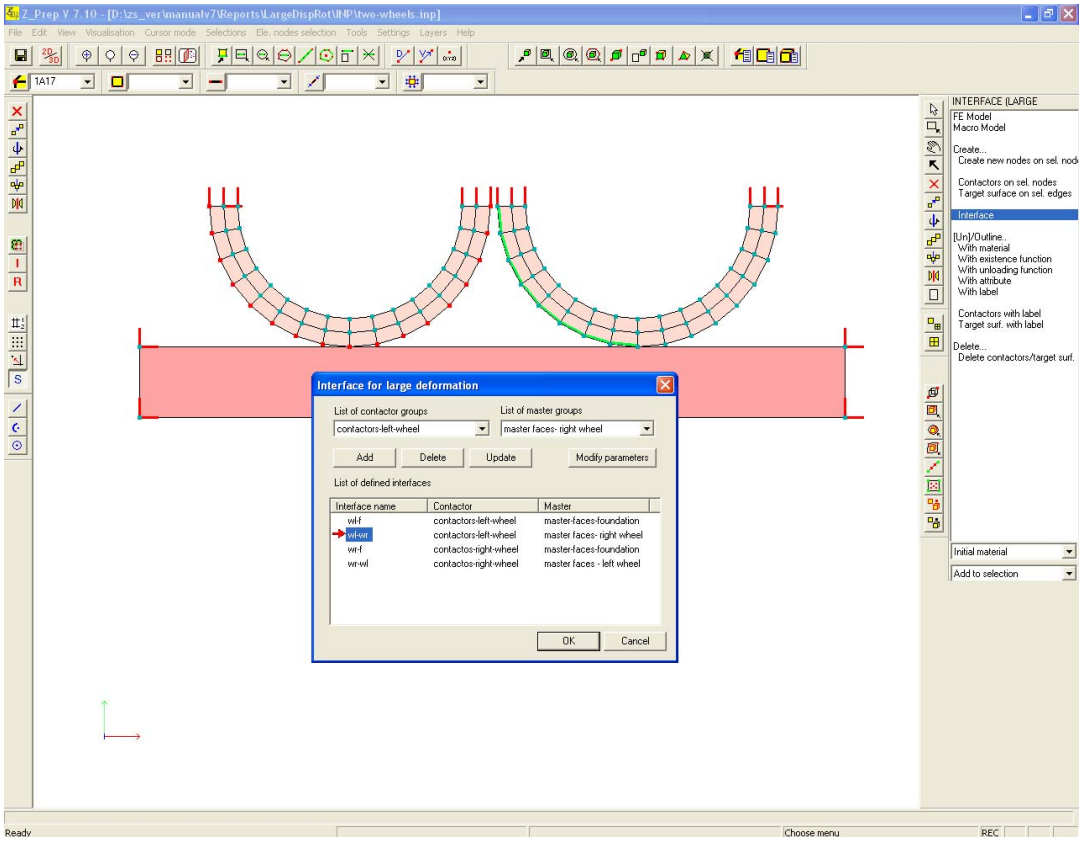

Figure 3.39: Generation of interface left wheel-right wheel

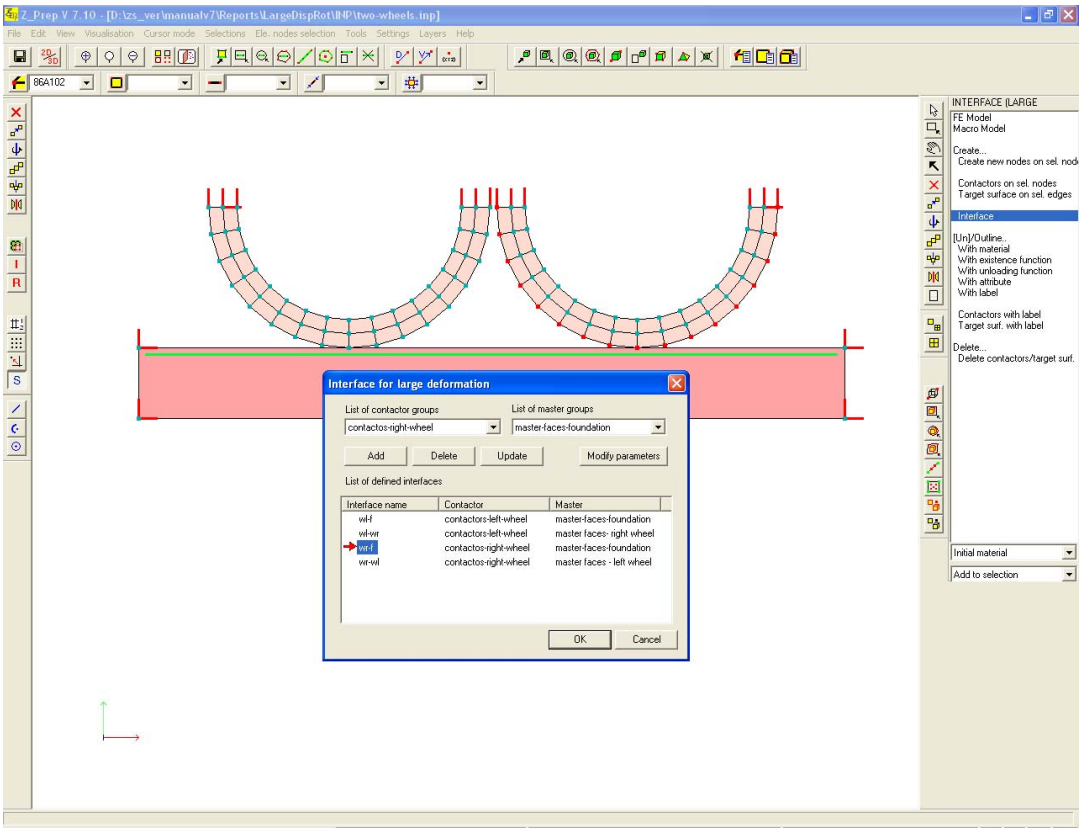

Figure 3.40: Generation of interface right wheel-foundation

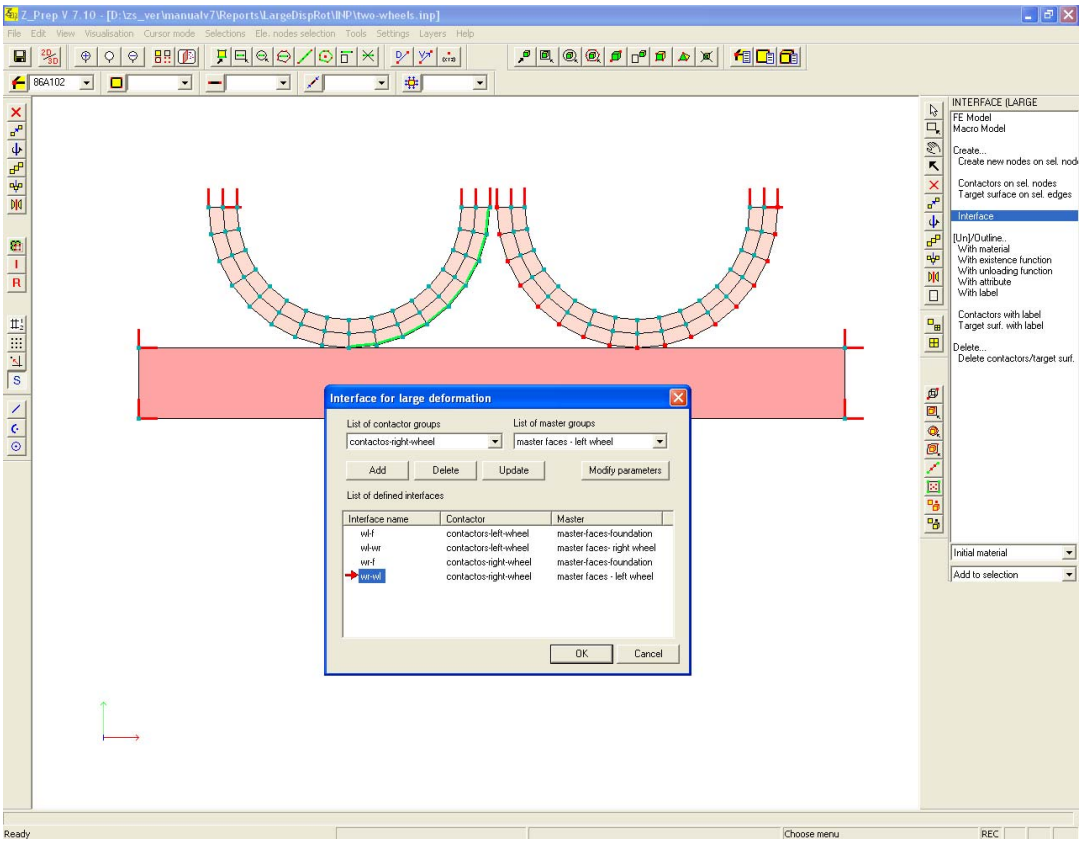

Figure 3.41: Generation of interface right wheel-left wheel

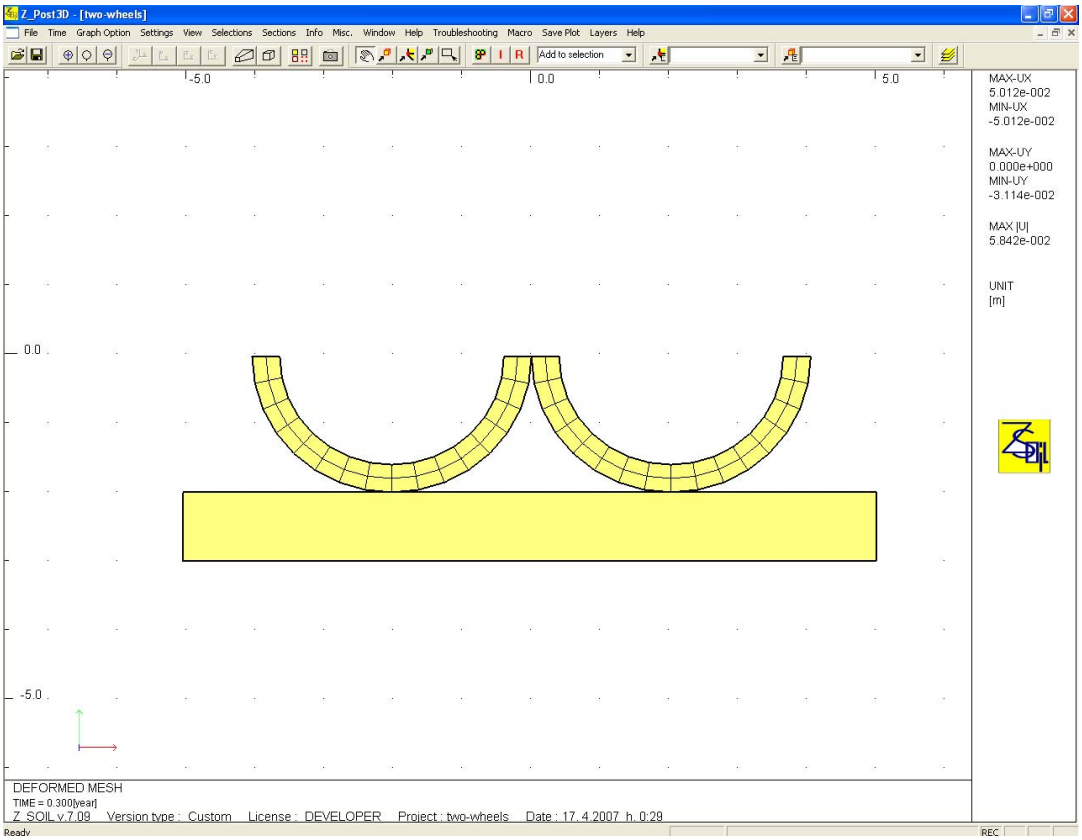

Figure 3.42: Deformation at stage of first contact of the two wheels

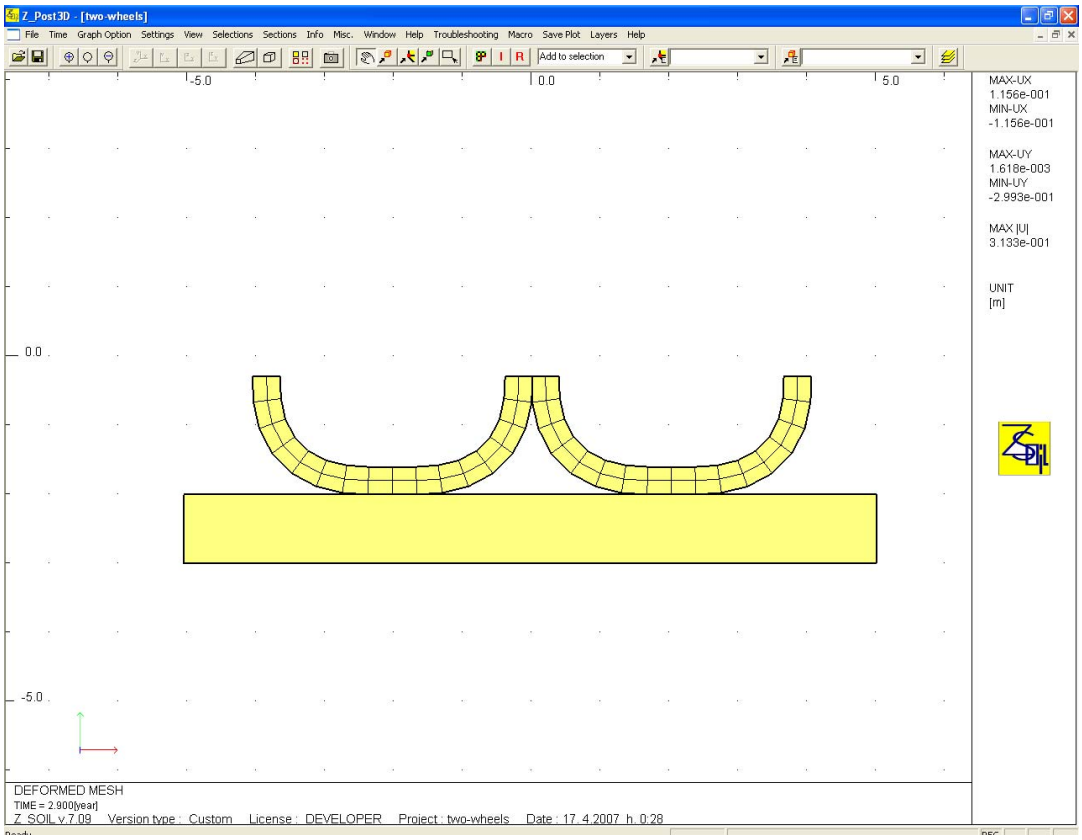

Figure 3.43: Deformation at stage of advanced contact of the two wheels

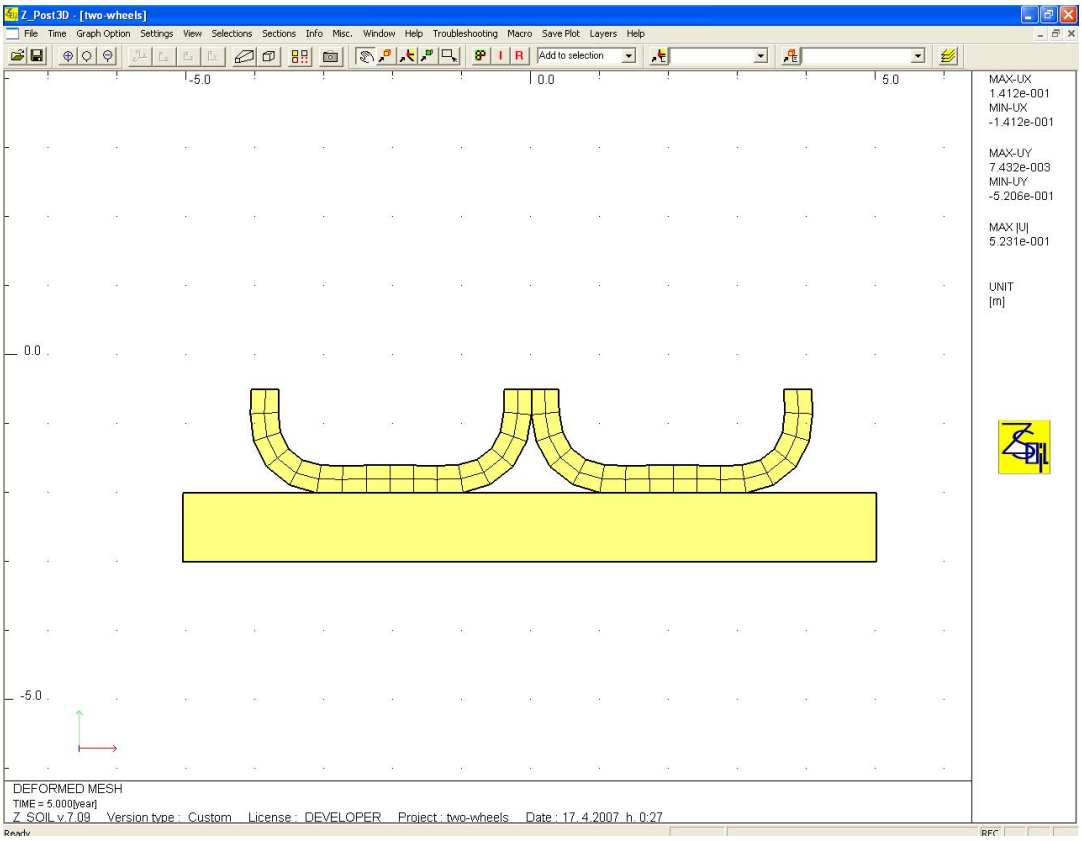

Figure 3.44: Deformation at stage of separation of the wheels from the foundation (at central point)

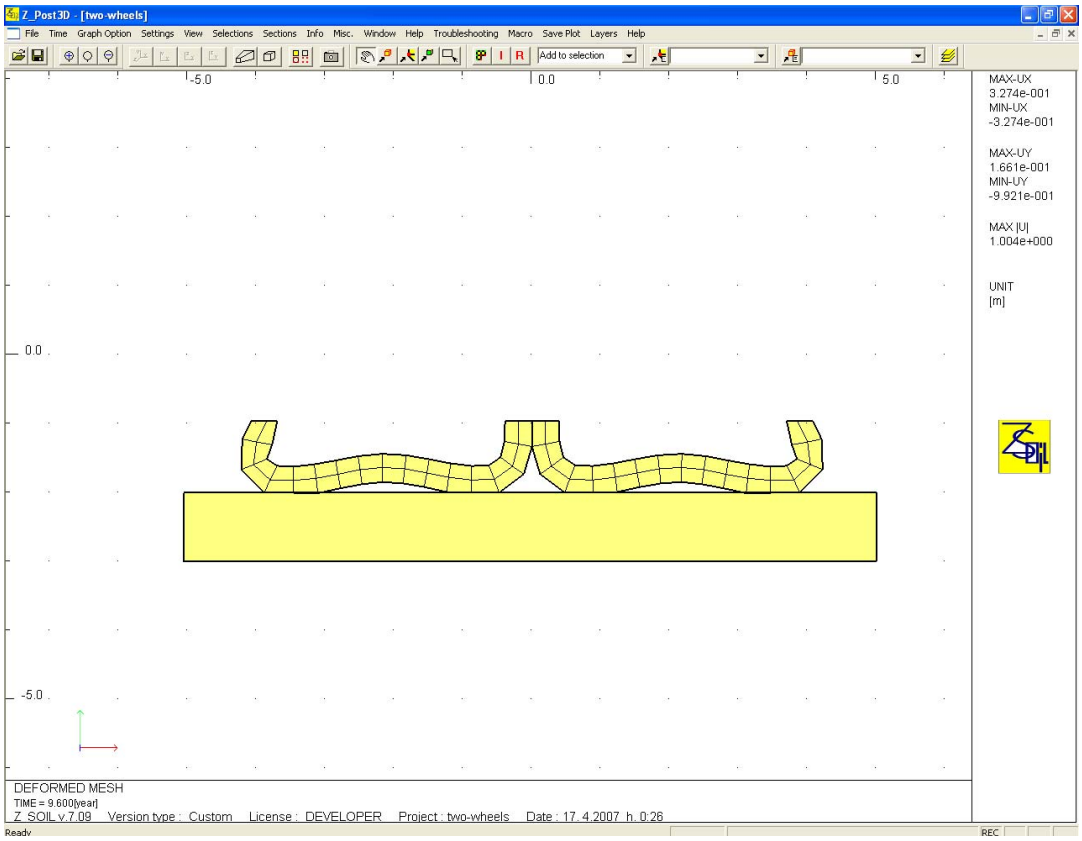

Figure 3.45: Deformation at stage of advanced separation of the wheels from the foundation

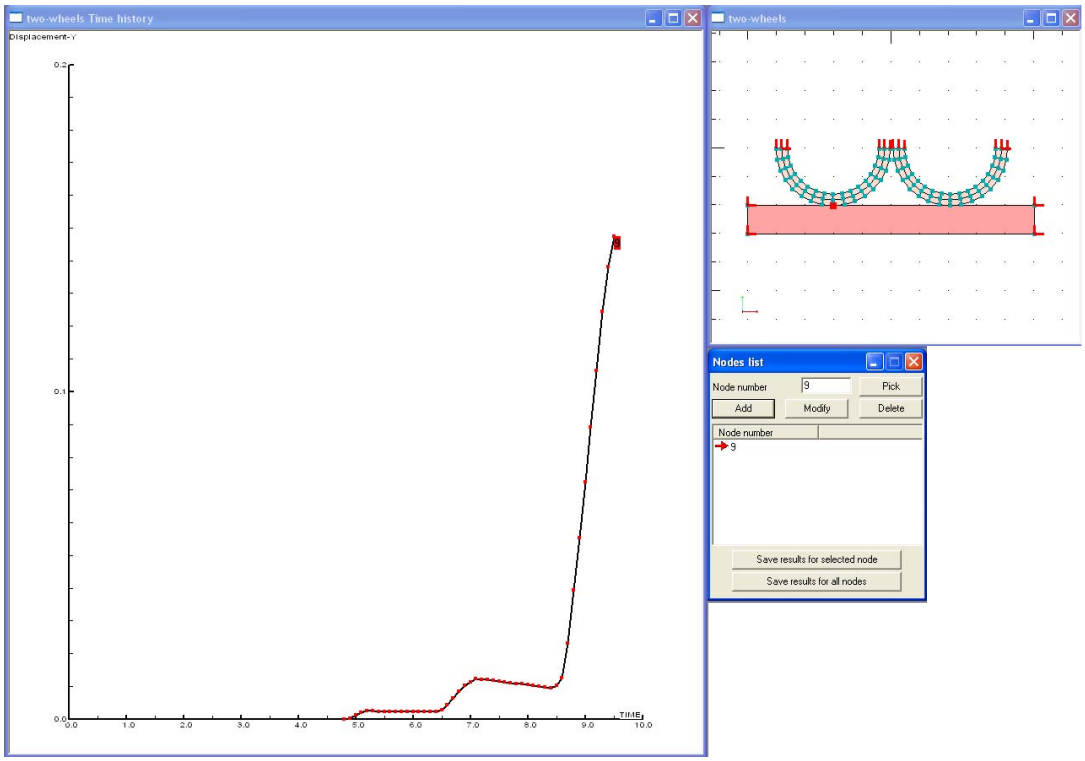

Figure 3.46: Evolution of vertical displacement

REFERENCES

1. C.C.Rankin and B.Nour-Omid: The use of projectors to improve finite element performance. (Computers & Structures ,1988)

2. C.C.Rankin and B.Nour-Omid: Finite rotation analysis and consistent linearization using projectors. (Computer Methods in Applied Mechanics and Engineering,1990)

3. M.A.Chrisfield and G.F.Moita: A unified co-rotational framework for solid shells and beams. (International Journal for Solids and Structures, 1996)

4. B.Skallerud and B.Haugen: Collapse of thin shell structures. Stress resultant plasticity modeling and finite element formulation. (International Journal for Numerical Methods in Engineering, 1999)

5. H. Parisch and Ch. Lübbing. A formulation of arbitrarily shaped surface elements for three-dimensional large deformation contact with friction. (International Journal for Numerical Methods in Engineering, vol. 40, p.3359-3383, 1997)

6. P. Papadopoulos and R. L. Taylor. A mixed formulation for the finite element solution of contact problems. Computer Methods in Applied Mechanics and Engineering 94 (1992) p. 373-389.

7. P. Litewka, P. Wriggers, J. Rakowski. 3D Beam finite element for large displacement analysis. Proceedings of ECCM 2001

8. M. Życzkowski (ed). Mechanika Techniczna t.IX, Wytrzymałość elementów konstrukcyjnych. p. 300. PWN Warsaw 1988.

9. J. Chróścielewski. Rodzina elementow skończonych klasy C0 w nieliniowej sześcioparametrowej teorii powłok. Zesz.Nauk Politechniki Gdańskiej Nr 53